

Greg Gibson
Vice President, Regulatory Affairs

750 East Pratt Street, Suite 1600
Baltimore, Maryland 21202



10 CFR 50.4
10 CFR 52.79

July 23, 2010

UN#10-207

ATTN: Document Control Desk
U.S. Nuclear Regulatory Commission
Washington, DC 20555-0001

Subject: UniStar Nuclear Energy, NRC Docket No. 52-016
Response to Request for Additional Information for the
Calvert Cliffs Nuclear Power Plant, Unit 3,
RAI 218 and RAI 229, Stability of Subsurface Materials and Foundations

- Reference:
- 1) Surinder Arora (NRC) to Robert Poche (UniStar Nuclear Energy), "FINAL RAI 218 RGS1 4332" email dated March 7, 2010
 - 2) Surinder Arora (NRC) to Robert Poche (UniStar Nuclear Energy), "FINAL RAI 229 RGS1 4566" email dated April 30, 2010
 - 3) UniStar Nuclear Energy Letter UN#10-177 from Greg Gibson to Document Control Desk, U.S. NRC, Response to Request for Additional Information for the Calvert Cliffs Nuclear Power Plant, Unit 3, RAI 218, Stability of Subsurface Materials and Foundations, Questions 02.05.04-05 and 02.05.04-13, dated June 30, 2010
 - 4) UniStar Nuclear Energy Letter UN#10-185 from Greg Gibson to Document Control Desk, U.S. NRC, Response to Request for Additional Information for the Calvert Cliffs Nuclear Power Plant, Unit 3, RAI 229, Question 02.05.04-20, Stability of Subsurface Materials and Foundations, dated July 9, 2010

The purpose of this letter is to respond to the requests for additional information (RAI) identified in the NRC e-mail correspondence to UniStar Nuclear Energy, dated March 07, 2010 (Reference 1), and April 30, 2010 (Reference 2). These RAIs addresses Stability of Subsurface Materials and Foundations, as discussed in Section 2.5.4 of the Final Safety Analysis Report

DDAL
NRC

(FSAR), as submitted in Part 2 of the Calvert Cliffs Nuclear Power Plant (CCNPP) Unit 3 Combined License Application (COLA), Revision 6.

References 3 and 4 anticipated that the responses to RAI 218 Questions 02.05.04-03, 2.05.04-08, 02.05.04-09 and 2.05.04-10 and RAI 229 Questions 02.05.04-17 and 02.05.04-19 would be provided to the NRC by July 23, 2010.

The enclosure provides our response to RAI 218 Questions 02.05.04-03, 02.05.04-09, 2.05.04-10, and an updated response to part 2 of Question 02.05.04-15; and our response to RAI 229 Questions 02.05.04-17 and 02.05.04-19.

UniStar Nuclear Energy requires additional time to finalize the response to RAI 218, Question 02.05.04-08. The response to this question will be provided by September 30, 2010.

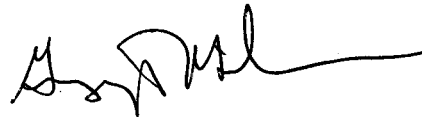
Our response does not include any new regulatory commitments and does not impact COLA content.

This letter does not contain any sensitive or proprietary information.

If there are any questions regarding this transmittal, please contact me at (410) 470-4205, or Mr. Wayne A. Massie at (410) 470-5503.

I declare under penalty of perjury that the foregoing is true and correct.

Executed on July 23, 2010



Greg Gibson

Enclosure: Response to NRC Request for Additional Information RAI 218 Questions 02.05.04-03, 02.05.04-09, 2.05.04-10 and 2.05.04-15 and RAI 229 Questions 02.05.04-17 and 02.05.04-19, Calvert Cliffs Nuclear Power Plant, Unit 3

cc: Surinder Arora, NRC Project Manager, U.S. EPR Projects Branch
Laura Quinn, NRC Environmental Project Manager, U.S. EPR COL Application
Getachew Tesfaye, NRC Project Manager, U.S. EPR DC Application (w/o enclosure)
Loren Plisco, Deputy Regional Administrator, NRC Region II (w/o enclosure)
Silas Kennedy, U.S. NRC Resident Inspector, CCNPP, Units 1 and 2
U.S. NRC Region I Office

Enclosure

Response to NRC Request for Additional Information

**RAI 218 Questions 02.05.04-03, 02.05.04-09, 2.05.04-10 and 2.05.04-15
and**

RAI 229 Questions 02.05.04-17 and 02.05.04-19,

Calvert Cliffs Nuclear Power Plant, Unit 3

RAI 218

Question 02.05.04-3

Section 2.5.4.5.2 indicates that most Category I structures will be founded on the top of Stratum IIb cemented sand layer. In Section 2.5.4.2.1.3, the layer IIb is further divided into three sublayers: silty sand layer with SPT N value greater than 20; clayey sand layer with N value smaller than 20; and poorly-graded sand to silty sand layer with N value greater than 20. The shear wave velocity of the layer IIb shows great variation, ranging from 560 to 3,970 ft/s. In addition, the shear strength property of the IIb is only based on very limited laboratory test results (one triaxial test for sublayer IIb-1 and two tests for sublayer IIb-2). Because the properties of the load-bearing layer IIb directly affect the foundation stability, the applicant is requested to explain how specific soil parameters for this layer were incorporated into relevant calculations (such as bearing capacity, settlement, SSI and GMRS), and discuss how the soil shear strength property for this layer was characterized based on limited testing results. In addition, describe how the variability was accounted for in the soil parameters for layer IIb in the above analyses.

Response

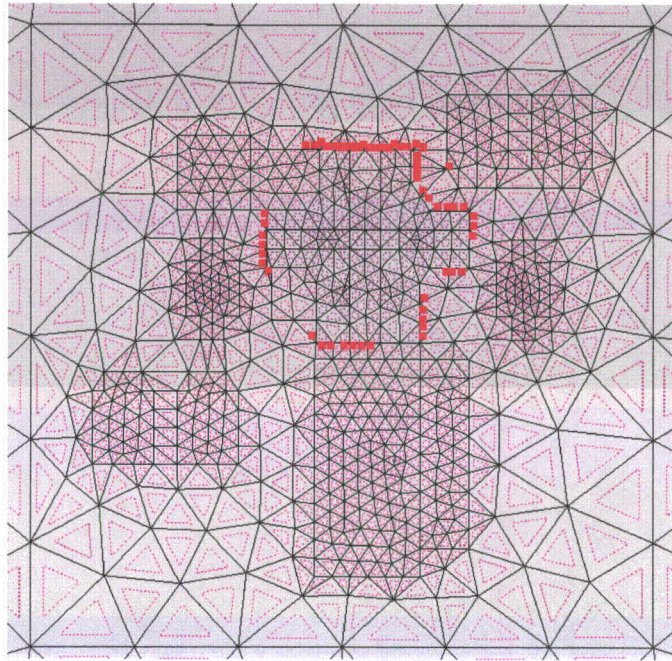
Soil properties were determined based on test results conducted for materials in Calvert Cliffs Nuclear Power Plant (CCNPP) Unit 3 powerblock area. If no information is available for the CCNPP Unit 3 powerblock area, results for the entire site were used. From the data selected, average values were calculated and used in the analyses. As mentioned in the question, data is limited particularly for shear strength of Layer IIb. However, the settlement calculations are not expected to be significantly impacted by the shear strength, since the deformation is observed mostly in the elastic range (Figure 1). The impact of the shear strength variability is further discussed in the response to RAI 218 Question 02.05.04-15 Part 2.

Lower bound analysis for other soil parameters is discussed in the response to RAI 229 Question 02.05.04-17 Part 3.

Analyses related to soil-structure interaction (SSI) and ground motion response spectra (GMRS) are sensitive to the selected best estimate of the shear wave velocity profile and the shear modulus and damping strain dependant degradation curves. The variability of shear wave velocity is analyzed in CCNPP Unit 3 FSAR Section 2.5.4 and further discussed in the responses to RAI 218 Question 02.05.04-15 Part 2 and to RAI 229 Question 02.05.04-17 Part 3. The development of the best estimate soil profile accounts for the totality of the measurements at the site. Amplification analysis to develop the GMRS incorporates random variability of the shear wave velocity profile. This approach covers the variability observed in the field. The strain dependant curves for shear modulus and damping were selected from site specific Resonant Column Torsional Shear (RCTS) tests and random variability is also incorporated within the amplification analysis. It is relevant to note that the GMRS at the CCNPP Unit 3 site presents a Peak Ground Acceleration (PGA) of 0.08 g and that the site specific safe shutdown earthquake (SSE) is a broad band spectra anchored at 0.15 g which almost doubles the GMRS. Soil-structure interaction is based on a deterministic analysis that uses three sets of strain dependant shear modulus and damping. These three sets result from the amplification analysis, which already incorporates the variability in shear wave velocity. In conclusion, the variability of the parameters that affect the estimation of the GMRS, SSE, and profiles for SSI has been accounted for in

the analyses in CCNPP Unit 3 FSAR Section 2.5.2 *Vibratory Ground Motion* and Section 3.7.1 *Soil Structure Interaction*.

Figure 1
Plastic Points at El. 41.5 ft On Top of Layer IIb-1



COLA Impact

Changes to the CCNPP Unit 3 COLA are not required as a result of this response.

RAI 218

Question 02.05.04-9

Section 2.5.4.2.5.2 summarizes chemical test results and concludes that "all natural soils at the site will be considered aggressive to concrete, requiring protection if placed within these soils." Since many Category I structures with concrete foundation will be built on Stratum IIb soil, please provide information on what measures will be taken to protect the concrete and if those measures will meet other design requirements, such as sliding coefficient parameter defined in the U.S. EPR standard design.

Response

Seismic Category I structures will be built on structural fill, which does not have the aggressive properties associated with the natural soils. However, in the powerblock area, the post-construction Surficial aquifer water table is approximately 30 feet below finished grade. The deep structures associated with the Nuclear Island will penetrate the water table and be exposed to the low pH groundwater. To protect the concrete, a waterproof lining system will be installed. The design of this system, including discussion of the coefficient of friction, is addressed in the response to RAI Nos. 144 and 145¹. Included with the response is a re-write of CCNPP Unit 3 FSAR Section 3.8 to discuss the liner system and design parameters, and a new departure in COLA Part 7 to address the coefficient of friction, which is less than the 0.7 as established in the U.S. EPR FSAR.

COLA Impact

Changes to the CCNPP Unit 3 COLA to address the waterproof membrane and the coefficient of friction of the soils are included in the response to RAI 144 and 145¹.

¹ UN#10-193, UniStar Nuclear Energy letter from Greg Gibson to Document Control Desk, U.S. NRC, Response to Request for Additional Information for the Calvert Cliffs Nuclear Power Plant, Unit 3, RAI No. 144, Other Seismic Category I Structures, and RAI No. 145, Foundations, dated July 23, 2010.

RAI 218

Question 02.05.04-10

Table 2.5-58 referred in Section 2.5.4.2.5.7 provides the sliding coefficient for each stratum with values ranging from 0.35 to 0.45. Since the U.S. EPR FSAR Tier II Section 2.5.4.3 "Foundation Interfaces" requires that a COL applicant will confirm that the site soils have sliding coefficient of friction equal to at least 0.7, please explain why lower than the standard design values were used in this application and evaluate the effect of lower sliding coefficients on structure sliding stability.

Response

Coefficients of surface friction provided in CCNPP Unit 3 FSAR Table 2.5-58 were obtained from "Foundations & Earth Structures"² for the soils at the site. These values were used in the evaluation of sliding stability in the response RAI Nos. 144 and 145¹. Included with the response is a re-write of CCNPP Unit 3 FSAR Section 3.8 and a new departure in COLA Part 7 to address the coefficient of friction, which is less than the 0.7 as established in the U.S. EPR FSAR.

COLA Impact

Changes to the CCNPP Unit 3 COLA to address the coefficient of friction of the soils are included in the response to RAI 144 and 145¹.

² Foundations and Earth Structures, Design Manual 7.02, Naval Facilities Engineering Command, pp 7.02-63, Table 1 [Report] - 1986

RAI 218

Question 02.05.04-15

Section 2.5.4.10.1 states that three cases were considered during bearing capacity calculations. For the general case, the bearing capacity equation for homogeneous soil was used by applying weighted average values of soil parameters in the analysis, with the weight factors based on the relative thickness of each stratum within a specific depth. For the case of a footing supported on a dense sand stratum over a soft clay stratum, Meyerhof's model (Meyerhof, et al., 1978) was used to estimate ultimate static bearing capacity. Since the results of the bearing capacity analysis were controlled by the models, assumptions and parameters, the applicant is requested to:

1. Provide details on how the weight factors were determined for all subsurface soil strata;
2. Clarify and justify if soil compressibility was considered during the analysis since a clayey sand layer (Layer IIb2) is presented;
3. Discuss whether the dimension of a structure will affect the analysis results for footing supported on a dense sand stratum overlying on a soft clay stratum, because the Meyerhof model is based on the assumption that one dimension of the rectangular foundation is much larger than the other. Also, please clarify why the equation of q_{ult} presented in page 2-1252 is different from Meyerhof's equation by a factor of 2.

Response

Note: This question was addressed in a previous UNE letter³. With respect to Part 2 of this question, UNE stated:

Soil compressibility was not considered during the analysis. Soil compressibility will be addressed in RAI Question 02.05.04-3 by introducing variability in compressible layer thickness and soil properties.

However, due to the magnitude of information presented on soil compressibility, this information is provided as a separate updated response to Part 2 of this question.

Part 2:

The ultimate static bearing capacity of the soil subsurface for all buildings was calculated using the following methods:

1. The model proposed by Vesic for footings supported on homogeneous soils. This method considers a homogeneous isotropic continuous medium underneath the foundation. Therefore, weighted average values of c' , ϕ' and γ' , based on the relative thickness of each stratum in the zone between the bottom of the foundation and a certain influence depth, were used in the calculations to obtain equivalent properties for the continuous medium. For this analysis, an influence depth of $1B$ was

³ UN#10-105, UniStar Nuclear Energy letter from Greg Gibson to Document Control Desk, U.S. NRC, Response to Request for Additional Information for the Calvert Cliffs Nuclear Power Plant, Unit 3, RAI No. 218, Stability of Subsurface Materials and Foundations, dated April 7, 2010.

considered to be adequate, where B is the building least lateral dimension. Two different cases are considered in the analysis:

- a) Soil subsurface including all strata: weighted average values of c' , ϕ' and γ' are used to obtain equivalent properties for the continuous medium.
 - b) Soil subsurface including only Stratum IIb Chesapeake Cemented Sand, with its corresponding three sublayers. Soil parameters of this layer are used to obtain equivalent properties for the continuous medium. For this case the depth of influence is considered to be the thickness of Stratum IIb, instead of $1B$.
2. The model proposed by Meyerhof for footings supported on a dense sand stratum over a soft clay stratum. Weighted average parameters of case b of the Vesic solution were used for the stiff sand layer and values corresponding to layer IIc Chesapeake Clay/Silt were used for the clay layer.

In order to verify the adequacy of the approach using weighted average soil strength parameters for the Vesic and Meyerhof models, a sensitivity analysis was performed. In this analysis, the results from the Vesic method are compared with two analytical models using Slope/W and Plaxis 2D software. The analytical models were developed considering the soil profile of the CCNPP Unit 3 Powerblock area and the corresponding soil strength properties for each layer. To account for the soil variability and limited information on soil strength parameters of some layers, lower bound parameters were used to calculate the bearing capacity. These lower bound soil parameters were determined based on lab testing available information and engineering judgment (See the response to RAI 229 Question 02.05.04-17 Part 3, for lower bound parameters evaluation). Table 1 and Table 2 present the soil properties used in the bearing capacity sensitivity analysis.

For the Vesic method, weighted average soil parameters based on layer thickness were used to obtain equivalent properties for the continuous medium. All strata within a depth of $1B$ were considered (case a).

The failure surfaces obtained using Slope/W software, for average and lower bound soil strength parameters, are shown in Figure 2 and Figure 3. The soil profile and strength properties listed in Table 1 and Table 2 were considered in the analysis. Ultimate bearing capacity was obtained by increasing the foundation load until failure was reached (i.e. a Factor of Safety (FOS) = 1.0). The Morgan-Price method was used in the calculations.

The depth of the slip failure surface is approximately $1B$ for the average parameters case, and it is reduced to approximately $0.93B$ for the lower bound case. Both values are in agreement with theoretical results and with the influence depth that was considered in the Vesic method.

In order to compare the results obtained with the Vesic method and Slope/W software, an analytical model was developed using Plaxis 2D software. The soil profile and strength properties listed in Tables 1 and 2 were considered in the analysis. The ultimate bearing capacity is obtained by an incremental load analysis; the load applied on the foundation was incremented with a predetermined load multiplier until a significant decrease in stiffness in the subsurface was observed.

The shear failure mechanism that is observed in the Plaxis 2D model (Figure 4 and Figure 5) is similar to the slip failure surface that was obtained with Slope/W. High shear stresses and total displacements occur beneath the foundation up to a depth of approximately $1B$. Results for the incremental analysis for average and lower bound soil strength parameters are shown in Figure 6 and Figure 7.

Ultimate and allowable bearing capacity results of the sensitivity analysis are presented in Table 3. The Vesic method provides the lower allowable bearing capacities, and Plaxis 2D provides the highest values. Results for average and also lower bound cases are above the minimum requirement for static loading of 22.0 ksf.

Figure 6 and Figure 7 show the results of ultimate bearing capacity for average and lower bound cases, respectively, obtained from Vesic close form solution, and Slope/W and Plaxis 2D. For Plaxis 2D, it was considered that the ultimate bearing capacity was reached when a significant decrease in stiffness was observed.

The sensitivity analysis shows that the Slope/W and Plaxis 2D models give similar ultimate bearing capacity results, which are higher than the results obtained with the Vesic method. Also, the failure mechanisms in both models are similar and in agreement with theoretical solutions (log-spiral shape). Therefore, the Meyerhof solution, where it is assumed that a layer of dense sand is overlaid by a layer of soft clay, results in a conservative approach to obtain the ultimate static bearing capacity of the NI at CCNPP Unit 3. The allowable static bearing capacity using Meyerhof solution reported in previous calculations is 23.5 ksf, which is lower than the value of 31.5 ksf obtained with Vesic method using lower strength bound parameters.

The sensitivity analysis on bearing capacity presented previously³ in the response to Part 1 of this question addresses the compressibility of the clayey sand sublayer IIb-2. In this analysis the results from Vesic close form solution, using weighted average strength parameters, are compared with two analytical models (Slope/W and Plaxis 2D). In these two models the soil profile and corresponding layer properties are considered. Therefore, the compressibility of clayey materials is included in the calculations.

The model proposed by Meyerhof assumes that a layer of dense sand is overlaid by a layer of soft clay in order to develop a punching failure mechanism where the stiffer layer (dense sand) is pushed into the lower softer layer (clay). For this analysis it was considered that Stratum IIb Chesapeake Cemented Sand corresponds to the dense sand layer and Stratum IIc Chesapeake Clay/Silt corresponds to the soft clay layer.

The equations recommended in the Meyerhof model that were used in the analysis are obtained from US Army Corps of Engineers, Technical Engineering and Design Guides, No. 7: "Bearing Capacity of Soils". Moreover, the information provided in this reference is based on the study performed by Hanna and Meyerhof⁴. Based on this publication, the following equation is recommended to estimate the ultimate bearing capacity for a strip footing of width B and depth D supported on a dense sand stratum over a soft clay stratum:

$$q_u = q_b + \gamma_1 H^2 \left(1 + \frac{2D}{H} \right) \frac{K_s \tan \phi_1}{B} - \gamma_1 H \leq q_t$$

⁴ A.M. Hanna and G.G. Meyerhof, "Design Charts for Ultimate Bearing Capacity of Foundations on Sand Overlying Soft Clay" Canadian Geotechnical Journal Volume 17, 1980.

However, the authors propose that this equation can be extended to circular footings as follows:

$$q_u = q_b + 2\gamma_1 H^2 \left(1 + \frac{2D}{H}\right) \frac{S_s K_s \tan \phi_1}{B} - \gamma_1 H \leq q_t$$

Where S_s varies between 1.1 and 1.27 and may be taken as unity, for conservative design; and B is the diameter of the circular foundation or width in case of a rectangular foundation.

Table 1
Stratum Thickness and Unit Weights used in the Bearing Capacity Calculation
CCNPP Unit 3 Powerblock Area

Stratum	Elevation (ft)		Thickness (ft)	Unit weight γ (pcf)		Effective unit weight γ' (pcf)	
	top	bottom		Average	lower bound	Average	lower bound
Structural fill	83.0	41.5	41.50	145	145	82.6	82.6
Stratum IIb-1 Chesapeake Cemented Sand	41.5	15.5	26.00	122	111	59.6	48.6
Stratum IIb-2 Chesapeake Cemented Sand	15.5	-7.5	23.00	123	111	60.6	48.6
Stratum IIb-3 Chesapeake Cemented Sand	-7.5	-23.5	16.00	123	117	60.6	54.6
Stratum IIc Chesapeake Clay/Silt	-23.5	-213.5	190.00	104	96	41.6	33.6
Stratum III Nanjemoy Sand	-213.5	-317.0	103.50	127	119	64.6	56.6

Table 2
Soil Strength Parameters used in the Bearing Capacity Calculation
CCNPP Unit 3 Powerblock Area

Stratum	C' (ksf)		ϕ' (deg)	
	Average	Lower bound	Average	Lower bound
Structural fill	0.00	0.00	40.00	40.00
Stratum IIb-1 Chesapeake Cemented Sand	0.60	0.30	34.00	26.00
Stratum IIb-2 Chesapeake Cemented Sand	0.52	0.26	32.00	27.00
Stratum IIb-3 Chesapeake Cemented Sand	0.22	0.11	32.00	28.00
Stratum IIc Chesapeake Clay/Silt	0.80	0.40	32.00	25.00
Stratum III Nanjemoy Sand	0.00	0.00	40.00	30.00

Note: In previous calculations for bearing capacity, effective cohesion for sandy layers (IIb) was conservatively not considered, i.e., $c' = 0$. However, for this sensitivity analysis the average and lower bounds based on available information are used. (See the response to RAI 229 Question 02.05.04-17 Part 3, this enclosure).

Table 3
Allowable Bearing Capacity Results – Sensitivity Analysis

CASE	Ultimate Bearing Capacity, q_{ult} (ksf)			Allowable Bearing Capacity, q_a (ksf)		
	Vesic	Slope/W	Plaxis 2D	Vesic	Slope/W	Plaxis 2D
Average	263.4	295.5	330.0	87.8	98.5	110.3
Lower Bound	94.5	135.9	140.0	31.5	45.3	46.7

Note: A factor of safety of FOS = 3.0 is considered for static bearing capacity. i.e., $q_a = q_{ult}/FOS$

Figure 2
Slope/W Bearing Capacity Failure Surface – Average Parameters

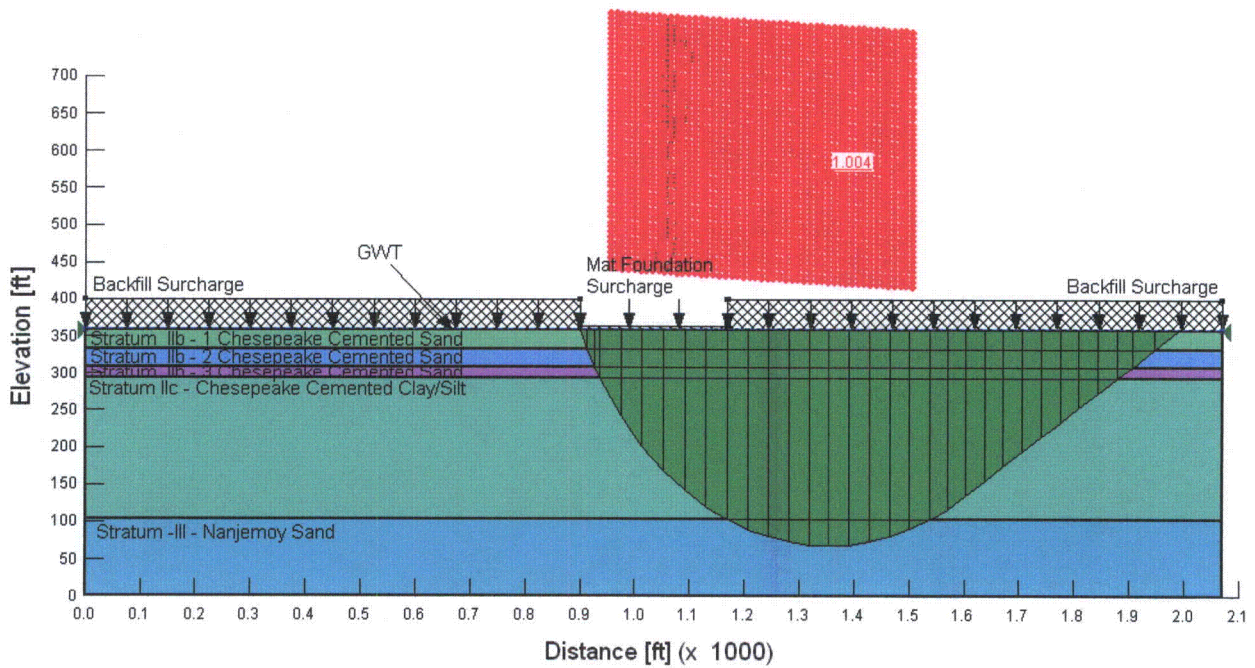


Figure 3
Slope/W Bearing Capacity Failure Surface – Lower Bound Parameters

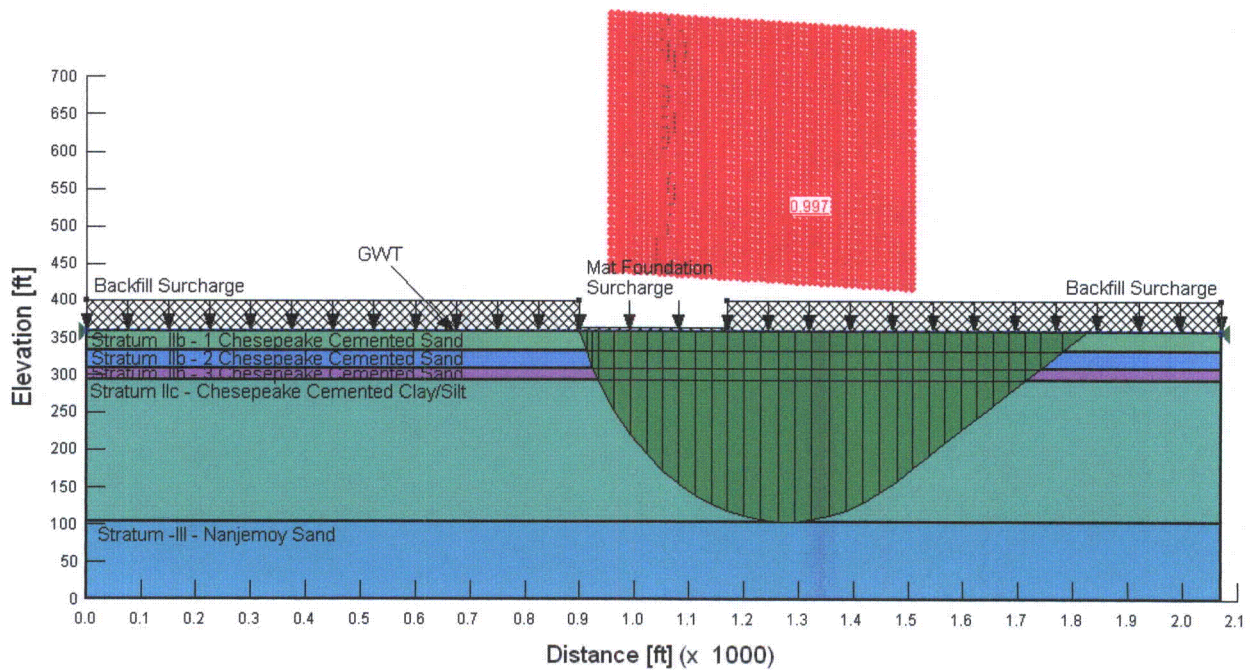


Figure 4
Plaxis 2D Analysis Results – Total Displacement Increments – Average Parameters

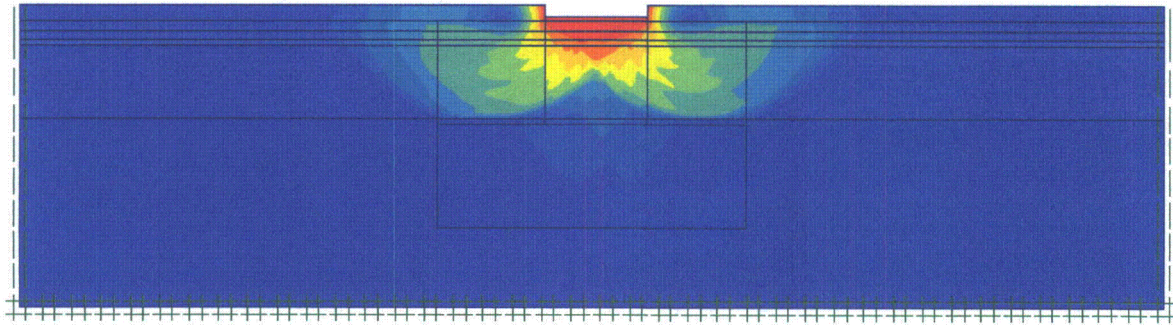


Figure 5
Plaxis 2D Analysis Results – Total Displacement Increments – Lower Bound Parameters

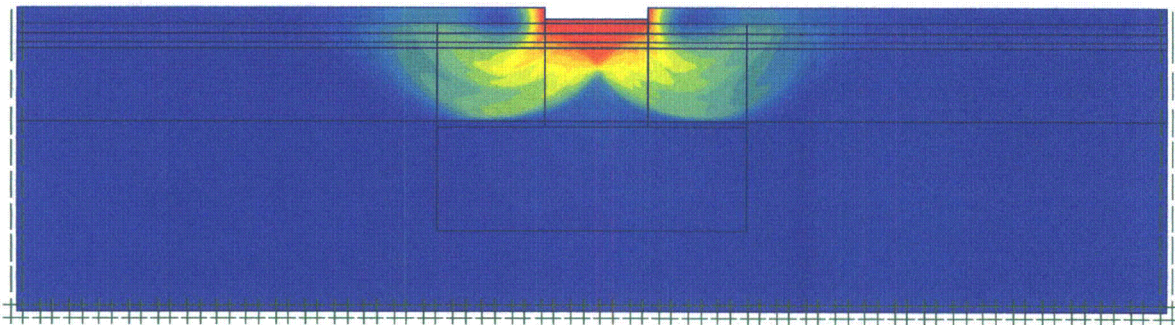


Figure 6
Ultimate Bearing Capacity Results – Average Parameters

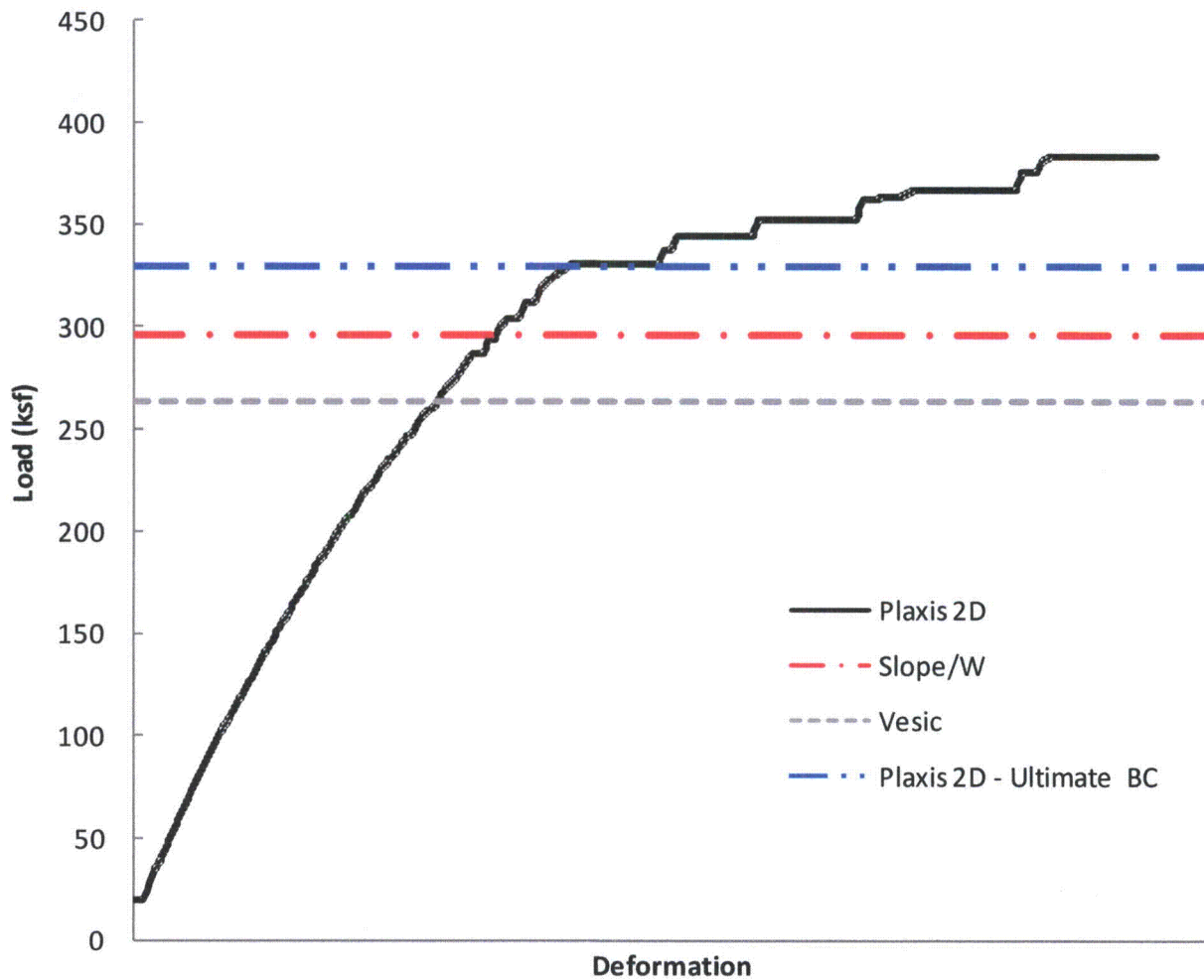
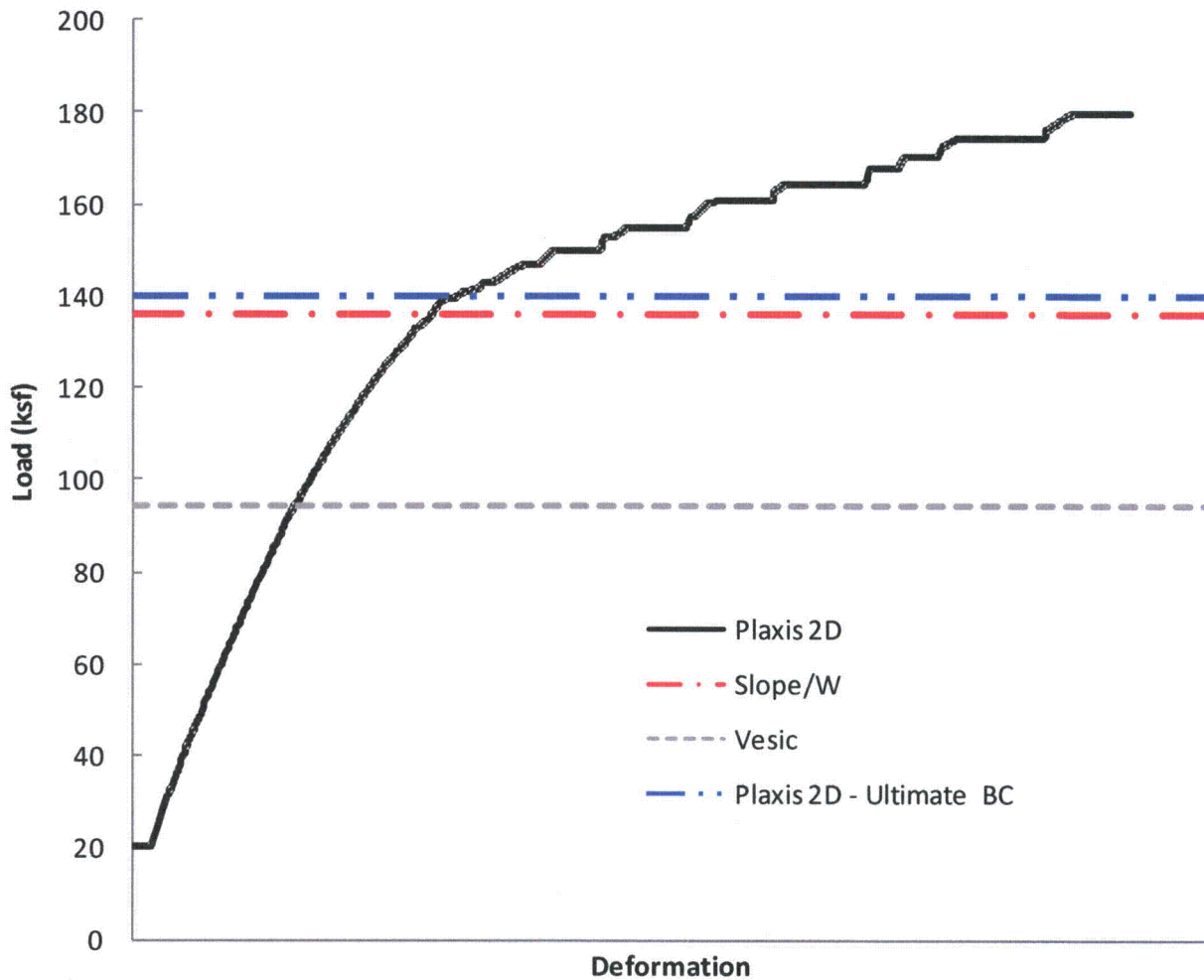


Figure 7
Ultimate Bearing Capacity Results – Lower Bound Parameters



COLA Impact

Changes to the CCNPP Unit 3 COLA are not required as a result of this response.

RAI 229

Question 02.05.04-17

FSAR Subsection 2.5.4.10.2.2 states that the initial effective stress conditions used in the FEM settlement model were in "accordance with the post-excavation overburden geometry" with an average surface elevation of 83 ft. In addition, the model assumed that excess pore water pressures created during excavation and dewatering are fully dissipated. It also presents the settlement analysis results, total and differential settlements for individual seismic Category I structures, based on a series of static loads applied to assimilate the assumed construction schedule, without consideration of dynamic loads created by seismic events.

1. Please explain the adequacy of the initial stress conditions selected in your FEM settlement calculation.
2. Please evaluate the possibility of any additional settlement caused by seismic event at the site.
3. Please address the effects of soil parameter variation and spatial variability on your settlement analysis.
4. Please address differential settlement between the nuclear island and adjacent structures, and compliance with the U.S. EPR standard design.
5. Please justify the assumptions, especially the determination of stress increases in each layer, used in the hand calculation of settlement you performed.

Response

Part 1:

Initial vertical effective stress distribution underneath/around a foundation directly affects the magnitude of foundation settlement. The vertical stress distribution is associated with the post-excavation geometry assuming that (a) excess pore pressure generated in Stratum IIc due to excavation is dissipated, and (b) excavation covers a large zone (1100 ft by 1100 ft). Following the excavation, stresses associated with unloading are induced at the excavation base (El. 41.5 ft). As a result of these stresses, heave is observed. As the immediate component of the heave takes place and the excess pore pressure due to excavation dissipates, the stress at the excavation base becomes close to zero. The excavation is expected to be completed in approximately 6 months, which is enough to dissipate at least 90% of the excess pore pressure due to the excavation. This forms the basis for the development of the 3D finite element model Middle Topography 2 (MT2) discussed in Section 2.5.4.10 of the CCNPP Unit 3 FSAR. The model assumes a flat ground surface at El. 83 ft, excavated to El. 41.5 ft, and loaded with structural fill and building loads. The adequacy of the stress conditions implemented in this model can be checked by developing another model that simulates the in situ initial topography more closely. To that end an independent model based on the Soil Hardening constitutive model (SH) has been developed. The excavated area of 1100 ft by 1100 ft is divided into three zones with different elevations, El. 60 ft, El. 80 ft, and El. 105 ft (Figure 8).

The SH model differs from MT2 model in the following ways:

- (a) Initial topography is flat for the MT2 model, and non-flat for the SH model.
- (b) The mesh for the SH model is finer.
- (c) The SH model adapts the Hardening Soil constitutive model, whereas the MT2 model utilizes Mohr Coulomb. The SH model can track the soil stiffness change as a function of stress changes, whereas MT2 model assumes a constant soil stiffness for all stresses.
- (d) The lateral stresses in SH model is calculated using overconsolidation ratios for each soil layer.

The SH model may be used to test the adequacy of the initial stress conditions implemented in the MT2 model. Figure 9 indicates the initial vertical stress distribution at the base of the excavation for both MT2 and SH models. As expected, the initial vertical stress (post-excavation) is around zero at the excavation base for both models. Figure 10 depicts the vertical stress distribution along the cross-section AA as given in Figure 9. Both models produce very similar initial vertical stress distributions.

As stated previously, the SH model utilizes the Hardening Soil constitutive model which varies the soil stiffness as a function of mean effective stress. In other words, differences in two lateral stress components may also impact the settlement results. Figure 11 shows the lateral stress components at the base of the excavation, where lateral stresses obtained from SH model are larger. The stiffness used by the MT2 model is not influenced by the magnitudes of lateral stresses, whereas the SH model uses these stresses to compute the mean effective stress and the soil stiffness.

The settlements obtained by MT2 and SH models are given in Figure 12 through Figure 14.

SH settlement predictions at the end of 8th step are in general less than MT2 settlement predictions. However, for some buildings, settlement prediction at the end of 5th loading step is larger according to SH model compared to that of MT2 model. This is due to fact that SH model assigns stiffness based on the stress level. As the mean effective stress underneath the foundation increases, the stiffness of the soil medium increases as well. This behavior can be captured by the SH model but not by the MT2 model.

This analysis indicates that MT2 model remains on the conservative side for the building center settlements except for the surface founded Emergency Power Generation Buildings (EPGBs). The structural fill underneath the EPGBs is 44.5 ft thick (= 76 - 41.5), and its placement is finished at the end of 4th step in the models, before the EPGB load is applied at the 5th step. Most of the EPGB displacement (more than 60%) is due to the fill. Before the EPGB construction begins, displacement in the fill would be leveled. In other words, the settlement estimates from the models are already conservative.

To account for the uncertainties involved in the estimation of soil parameters and spatial soil variability, the MT2 model results provided in the Section 2.5.4.10 of the CCNPP Unit 3 FSAR will be used. In addition, since settlement in the SH model produced similar results to the MT2 model, calculation of NI tilt based on the difference between the low topography and high topography model will be removed

Figure 8
Three Zoned Initial Topography,
El. 60 ft for Zone I, El. 80 ft Zone II, and El. 105 ft for Zone III.

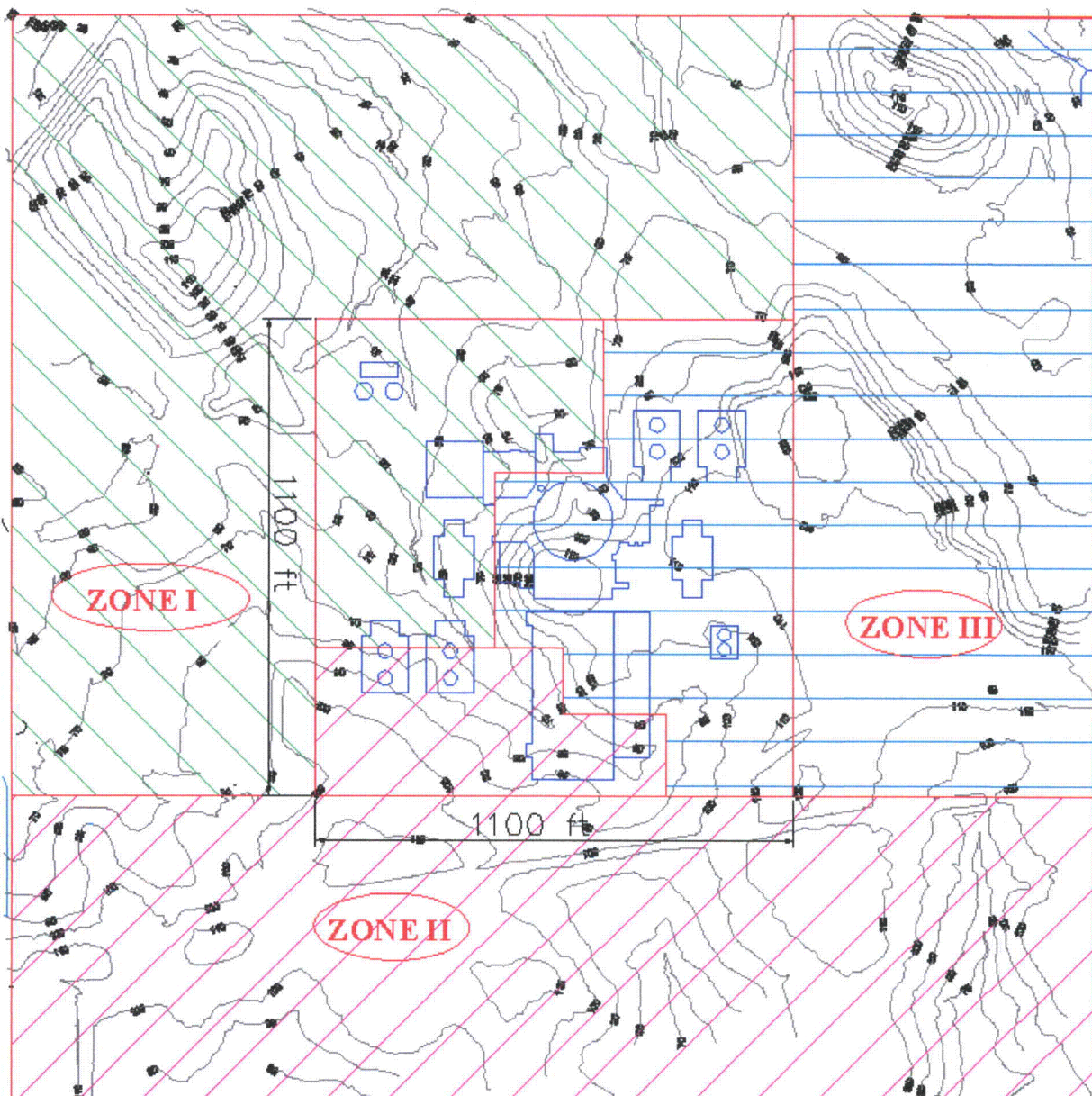


Figure 9
Effective Vertical Stress σ_{yy} Distribution at the Excavation Base for MT2 and SH Models.

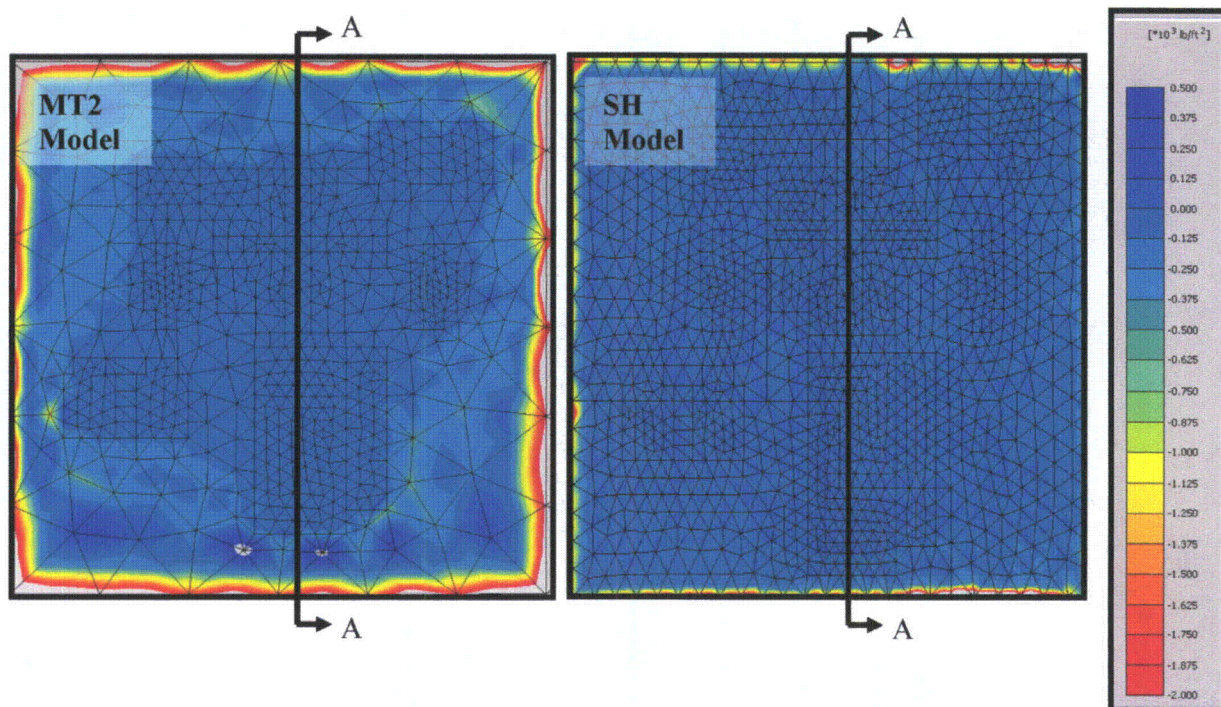


Figure 10
Effective Vertical Stress σ_{yy} Distribution for MT2 and SH Models
across Cross-Section AA.

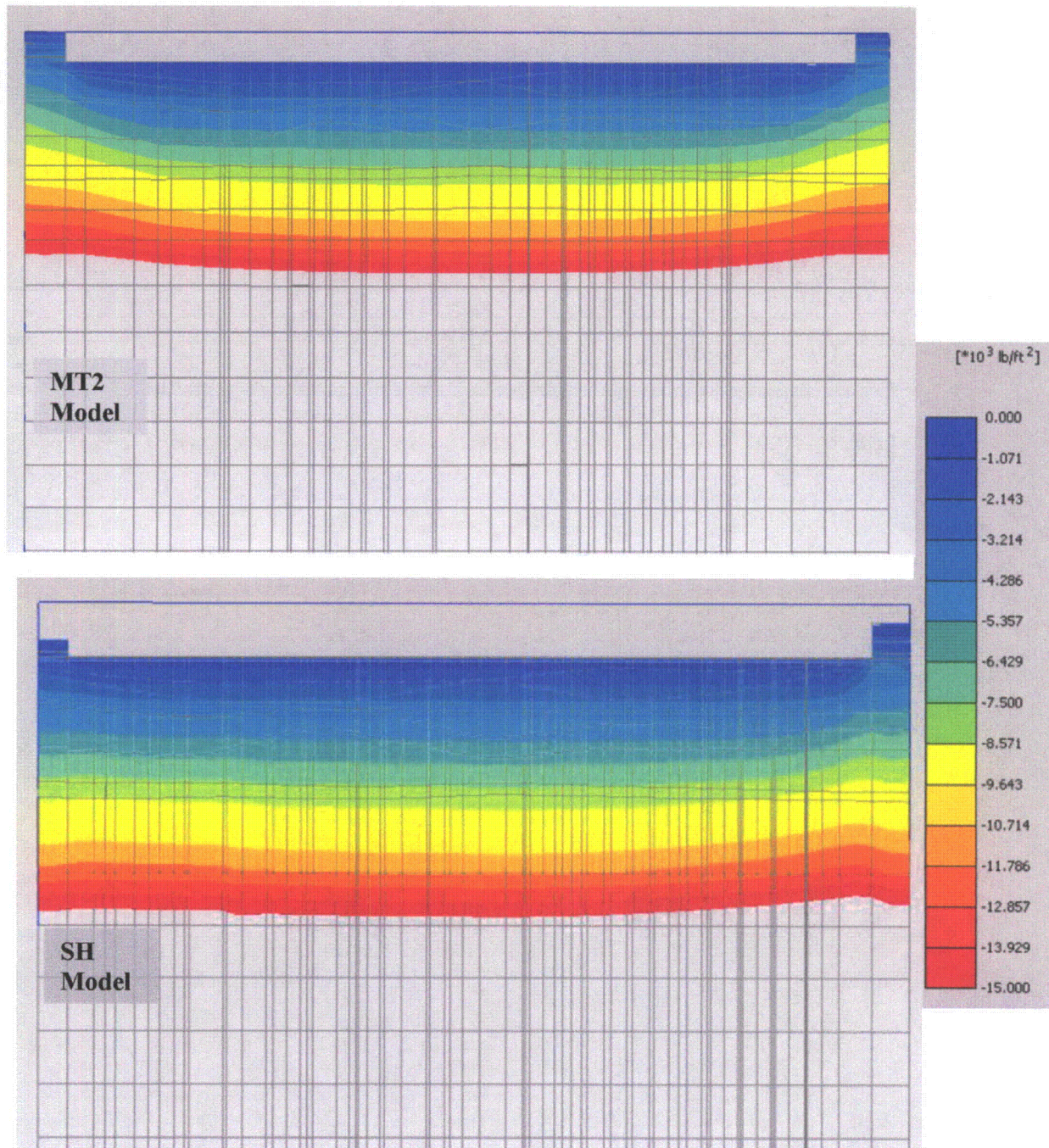


Figure 11
Effective Lateral Stresses σ_{xx} and σ_{zz} Distribution at the Excavation Base for MT2 and SH Models

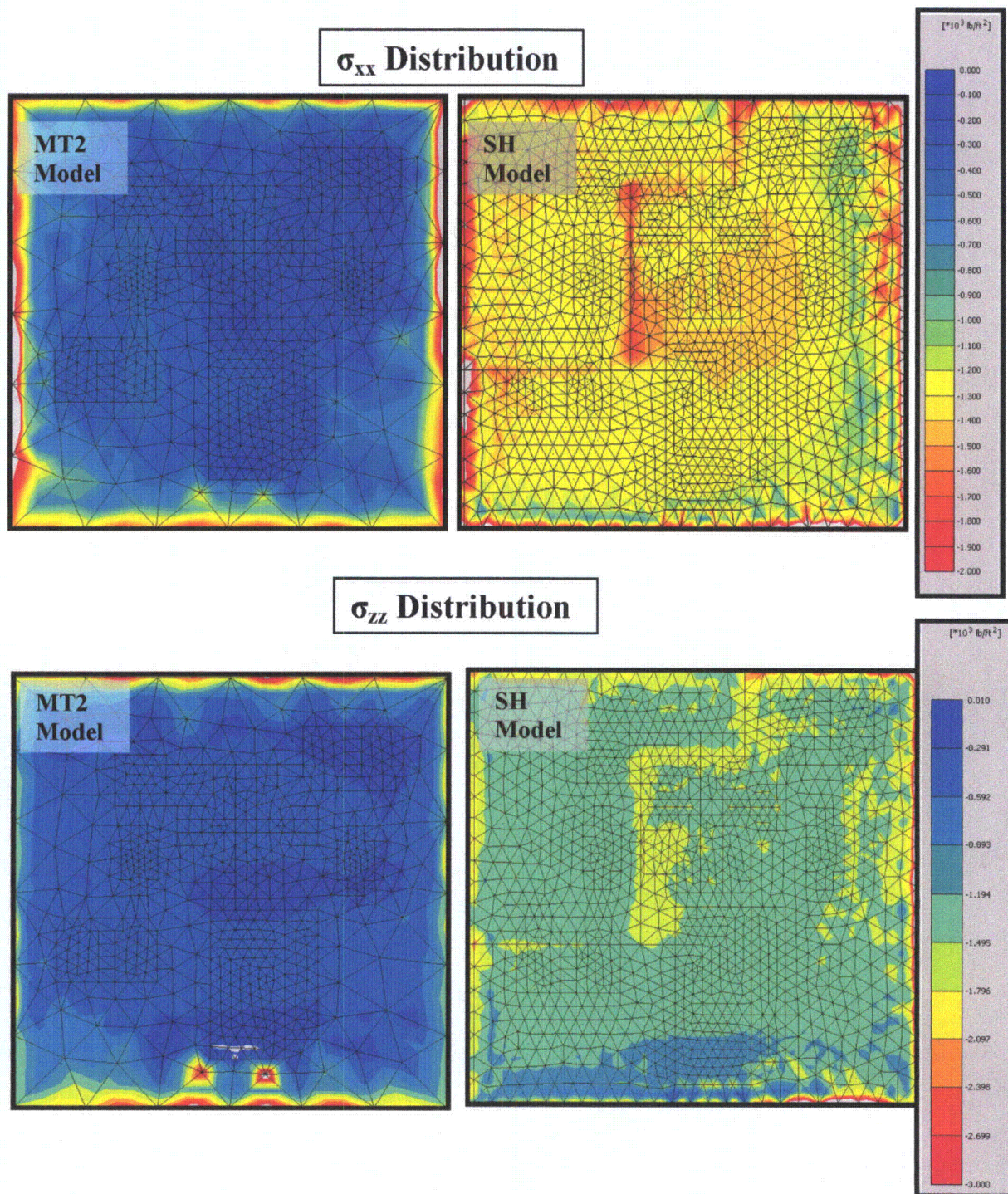


Figure 12
Center Settlements for Buildings: Reactor Building (RB), Fuel Building (FB), Safeguard Buildings (SGB1, SGB23, and SGB4).

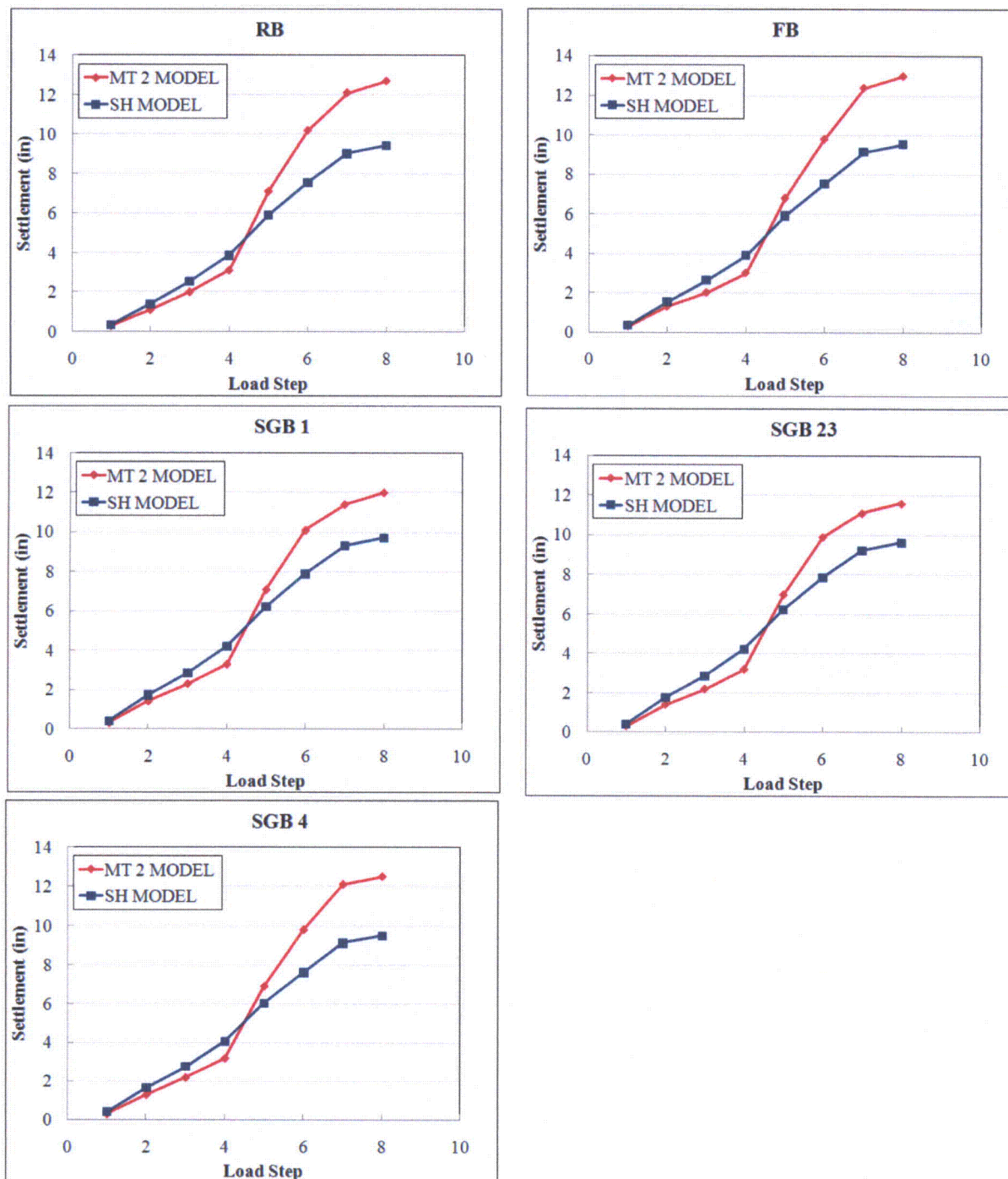


Figure 13
Center Settlements for Buildings: Nuclear Auxiliary Building (NAB), Access Building (AB),
Radwaste Processing Building (RWPB).

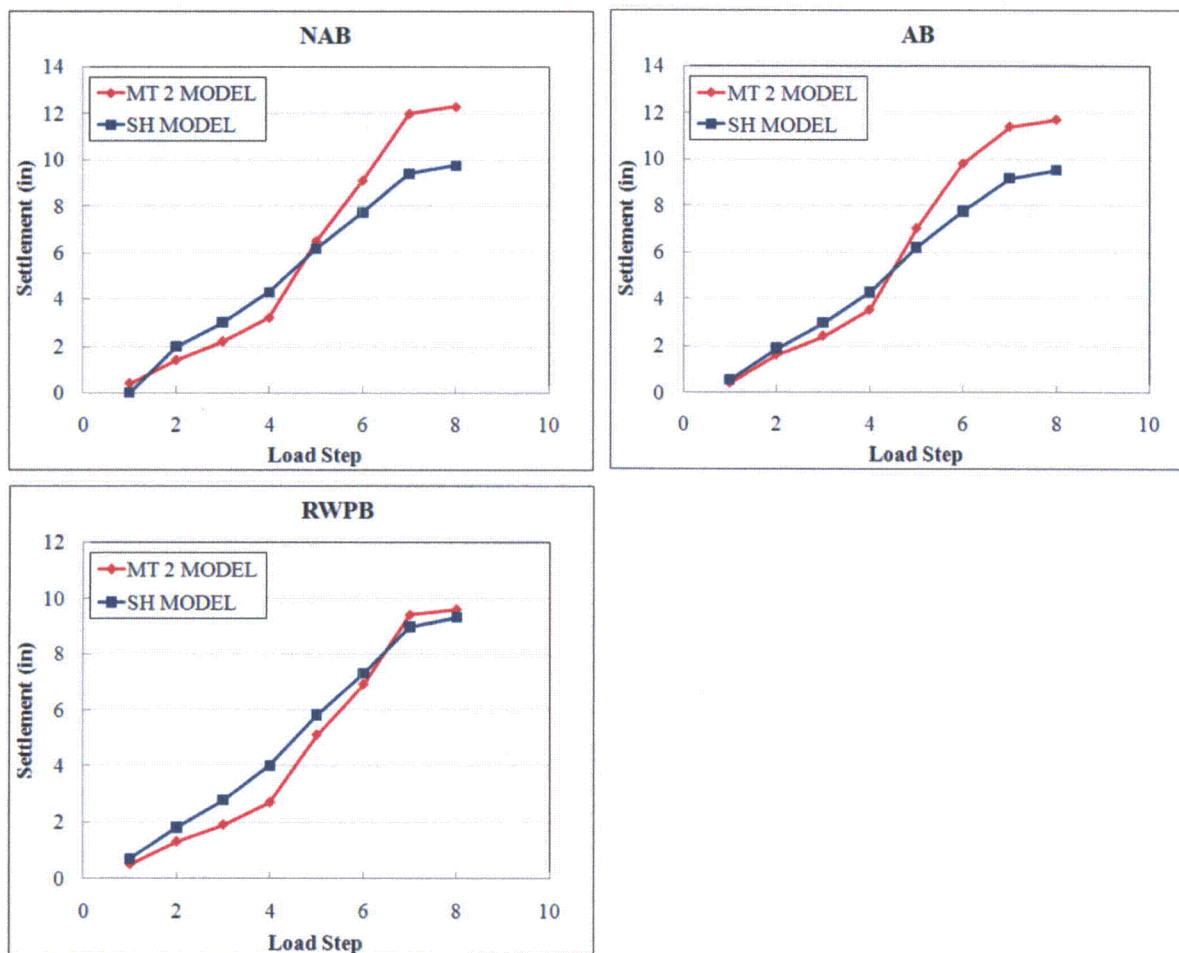
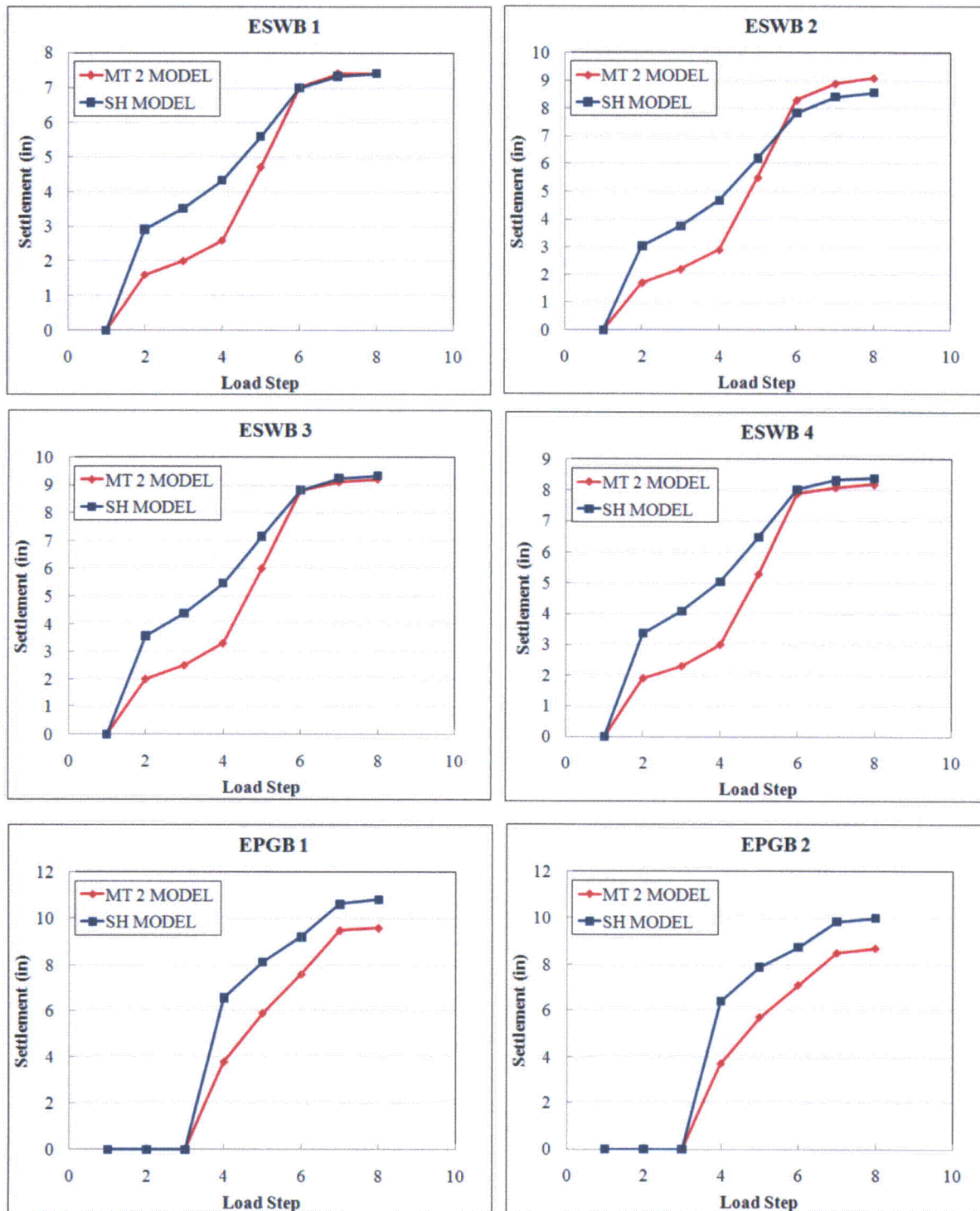


Figure 14
Center Settlements for Buildings: Emergency Service Buildings (ESWB1, ESWB2, ESWB3, ESWB4), Emergency Power Generator Buildings (EPGB1, EPGB2).



Part 2:

Additional settlement caused by a seismic event was calculated using approaches described by Tokimatsu and Seed⁵ and Lee⁶. These methodologies were developed for sandy soils. For clay/silt layers (Stratum IIa and Stratum IIc), the methodology described in Boulanger and Idriss⁷ was adopted for the potential deformation due to seismic excitation. It is indicated by Boulanger and Idriss⁷ that fine-grained soils with Plasticity Index (PI) greater than 12 percent are not susceptible to liquefaction and related seismic deformation. The soil index tests from CCNPP Unit 3 have shown that the PI is 36.6% percent and 41.6% for Stratum IIa and Stratum IIc, respectively. Therefore, no liquefaction and associated settlement is expected from Stratum IIa and Stratum IIc.

As a conservative approach, the depth of the groundwater table is considered at ground surface during the seismic settlement calculations.

Both approaches provide an estimate of volumetric strain due to seismic event based on the cyclic stress ratio $CSR_{7.5}$ and SPT blow counts corrected for hammer energy efficiency and overburden stress $(N_1)_{60}$. The cyclic stress ratio is calculated for an equivalent earthquake magnitude of 7.5. The $CSR_{7.5}$ expression used in the calculation is as follows:

$$CSR_{7.5} = 0.65 \left(\frac{\sigma_v}{\sigma'_v} \right) \left(\frac{a_{max}}{g} \right) \frac{(r_d)}{MSF}$$

where σ'_0 is the effective overburden pressure, σ_0 is the total overburden pressure, a_{max} is the maximum horizontal acceleration, which is 0.15g for CCNPP Unit 3, and r_d is the stress reduction factor calculated based on the expressions given by Youd⁸. MSF is the earthquake magnitude scaling factor. An earthquake magnitude of 6.0 is used in the seismic settlement analysis based on available information from CCNPP Unit 3 FSAR Section 2.5.4. The earthquake magnitude scaling factor (MSF) was calculated by following expression given by Lee⁶:

$$MSF = 2.5 - 0.2M$$

Where M is site earthquake magnitude as 6.0. MSF is given as 1.32 for earthquake magnitude 6.0 by Tokimatsu and Seed⁵.

The volumetric strain (ε_c) due to the seismic event was calculated by using the Figure 15 given by Tokimatsu and Seed⁵.

⁵ Tokimatsu, K. and Seed, H.B. (1987) "Evaluation of settlements in sand due to earthquake shaking". Journal of Geotechnical Engineering, ASCE. Vol. 113(8): 861-878.

⁶ Lee, C. Y. (2004), "Earthquake-Induced Settlements in Saturated Sandy Soils", ARPN Journal of Engineering and Applied Science, Editorial Asian Research Publishing Network (ARPN), August 2007.

⁷ Boulanger, R. W. and Idriss, I. M. (2004), "Evaluating the potential for liquefaction or cyclic failures of silts and clays. Report UCD/CGM-04/01, Center for Geotechnical Modeling, University of California, Davis, CA.

⁸ Youd, T. L. et al., (2001) "Liquefaction Resistance of Soils: Summary Report from the 1996 NCEER and 1998 NCEER/NSF Workshops on Evaluation of Liquefaction Resistance of Soils", Journal of Geotechnical and Geoenvironmental Engineering.

Similarly, the volumetric strains were calculated based on the following expression used by Lee⁶:

$$\varepsilon_c = 10[(N_1)_{60}]^{-0.6}$$

for cases where $\left(\frac{CSR}{(N_1)_{60}}\right) > 0.01$.

The total settlement (S) is obtained multiplying the volumetric strain of each layer by its corresponding thickness as:

$$S = \sum_{i=1}^n H_i \varepsilon_c$$

Based on the methodology described above, no seismic settlement is expected at the CCNPP Unit 3 site. The calculation spreadsheets are included as Table 4 and Table 5.

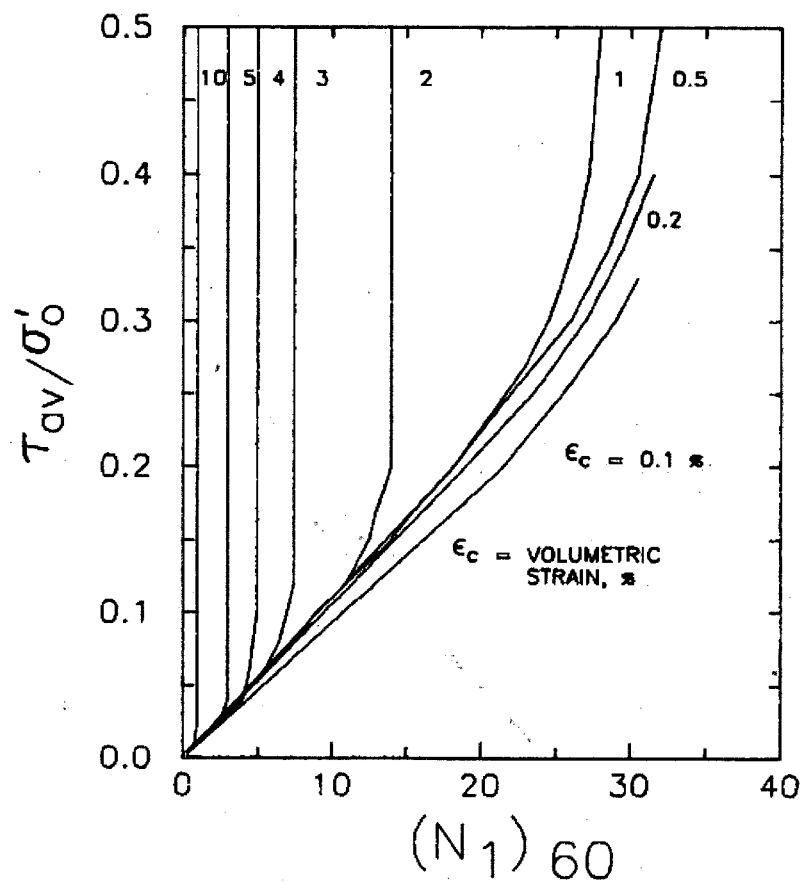
Table 4, Settlement Analysis Based on Tokimantsu and Seed⁵

Soil Layer	Depth [ft]	Thickness [ft]	Midpoint Thickness [ft]	Y _{moist} [pcf]	w [%]	Y _{dry} [pcf]	e	Y _{sat} [pcf]	σ ₀ [TSF]	u [TSF]	σ' ₀ [TSF]	N ₆₀	C _N	(N ₁) ₆₀	r _d	τ _{av} /σ' ₀	[τ _{av} /σ' ₀] _M	ε _c [%]	S [in]
	0.0	0.0	0.0					0			0.0								
Stratum I, Terrace Sand	28.0	28.0	14.0	121	15.8	104	0.85	133	0.9	0.4	0.5	14	1.45	20	0.9347	0.1715	0.1299	0.00	0.0
Stratum IIb, Chesapeake Cemented sand, Layer 1	71.0	24.0	12.0	122	24.1	98	0.80	126	3.8	1.8	1.9	89	0.74	66	0.6000	0.1141	0.0864	0.00	0.0
Stratum IIb, Chesapeake Cemented sand, Layer 2	94.0	23.0	11.5	123	30.5	94	0.80	122	5.2	2.6	2.6	24	0.63	15	0.6000	0.0788	0.0597	0.00	0.0
Stratum IIb, Chesapeake Cemented sand, Layer 3	110.0	16.0	8.0	123	26.0	98	0.64	122	6.4	3.2	3.2	63	0.57	36	0.6000	0.0541	0.0410	0.00	0.0
Stratum III, Nanjemoy Sand	411.0	108.0	54.0	127	29.1	98	1.00	130	20.7	11.1	9.6	75	0.33	25	0.6000	0.0000	0.0000	0.00	0.0

Table 5, Settlement Analysis Based on Lee⁶

Soil Layer	Depth [ft]	Thickness [ft]	Midpoint Thickness [ft]	Y _{moist} [pcf]	w [%]	Y _{dry} [pcf]	e	Y _{sat} [pcf]	σ ₀ [TSF]	u [TSF]	σ' ₀ [kPa]	σ' ₀ [TSF]	N ₆₀	C _N	(N ₁) ₆₀	r _d	CSR _{7.5}	CSR/(N ₁) ₆₀ >0.01	Conditional	ε _v [%]	S [in]
	0.0	0.0	0.0					0			0	0.0									
Stratum I, Terrace Sand	28.0	28.0	14.0	121	15.8	104	0.85	133	0.9	0.4	47	0.5	14	1.45	20	0.9347	0.1319	0.00649	Lower than 0.001	1.64	0.0
Stratum IIb, Chesapeake Cemented sand, Layer 1	71.0	24.0	12.0	122	24.1	98	0.80	126	3.8	1.8	183	1.9	89	0.74	66	0.6000	0.0883	0.00134	Lower than 0.001	0.81	0.0
Stratum IIb, Chesapeake Cemented sand, Layer 2	94.0	23.0	11.5	123	30.5	94	0.80	122	5.2	2.6	253	2.6	24	0.63	15	0.6000	0.0889	0.00589	Lower than 0.001	1.96	0.0
Stratum IIb, Chesapeake Cemented sand, Layer 3	110.0	16.0	8.0	123	26.0	98	0.64	122	6.4	3.2	308	3.2	63	0.57	36	0.6000	0.0895	0.00249	Lower than 0.001	1.17	0.0
Stratum III, Nanjemoy Sand	411.0	108.0	54.0	127	29.1	98	1.00	130	20.7	11.1	919	9.6	75	0.33	25	0.6000	0.0972	0.00393	Lower than 0.001	0.00	0.0

Figure 15
Relationship of Cyclic Stress (τ_{av}/σ'_0)_{7.5} [CSR_{7.5}], (N_1)₆₀ and Volumetric Strain (ϵ_c)



Part 3:

Soil Parameter Variation

The variability of the soil parameters on horizontal planes was assessed by comparing the soil parameter measurement at a given elevation at different horizontal locations around the site. The shear wave velocity, SPT blow count, water content, and plasticity index measurements obtained from various locations around the site were utilized for this assessment. These measurements were not conducted exactly at the same elevation, thus, a reference elevation was selected within the critical soil layers and the data points with a tolerance of up to ± 5 ft were used to compare the variability of particular measurement on horizontal plane.

The site was divided into six zones, Zone 1 to Zone 6 (Figure 16). The measurements in each zone were compiled and the change in each soil parameter was compared with the measurements from other zones. The results from the zones that are distant from each other (e.g., Zone 1 and Zone 6) provide the level of soil parameter variability throughout the power block area.

a. Shear Wave Velocity Distribution

The variation of shear wave velocity as a function of location on the horizontal plane, at a given elevation, is illustrated in Figure 17. Data from five borings were used in the analysis. Reference elevations were El. 50 ft for Stratum IIa, El. 25 ft for Stratum IIb-1, El. 0 ft for Stratum IIb-3, El. -25 ft for Stratum IIc-1, El. -50 ft Stratum IIc-2, El. -100 ft for Stratum IIc-3. Deviations from these reference elevations were limited to ± 1 ft.

For all layers, except for Stratum IIb-3, Figure 17 indicates that the variation within Zone 4 is almost the same as the variation between Zone 1, Zone 4, and Zone 6. This implies that the shear wave velocity is independent of horizontal location. For Stratum IIb-3, the shear wave velocity is high in Zone 1 according to data from boring B323. However, this is based on only one data point that could be spurious.

b. SPT Blow Counts Distribution

Figure 18 shows the variation of SPT blow counts corrected for energy efficiency N_{60} for different borings at given elevations. The analysis was conducted at mid-elevations of Layers IIb-1, IIb-2, IIb-3, and IIc. According to Figure 18, N_{60} is highly variable at a given elevation for all layers. Furthermore, no distinct correlation between zone number and N_{60} can be deduced from Figure 18. Specifically, for layer IIb-3, the change in shear wave velocity (high in Zone 1 lower in Zone 6) contradicts with change in N_{60} (low in Zone 1 and higher in Zone 6). This comparison excludes the outliers. As a conclusion, the scatter in N_{60} cannot be explained using the horizontal location in the power block area. Alternative explanation for the scatter within each zone and all zones in general may be the inherent scatter (aleatory uncertainty) involved in SPT testing procedure, and fluctuations in overburden stress, and groundwater elevation. The effect of overburden stress and groundwater elevation can be considered by looking at stress corrected blow counts as $(N_1)_{60}$. Figure 19 shows the $(N_1)_{60}$ variation for borings considered in Figure 18. $(N_1)_{60}$ distribution is more uniform at a given elevation

compared to N_{60} distribution since the scatter due to overburden stress and groundwater elevation is implicitly reduced by $(N_1)_{60}$ evaluation. The scatter observed in Figure 19 for a given layer at a given elevation is attributed to the inherent scatter involved in SPT testing procedure on site. Again, the scatter does not seem to be a function of the zone number.

c. Water Content and Plasticity Index Distribution

Soil index properties such as water content and plasticity index (PI) distribution impact the measured shear wave velocity and N_{60} . The water content and PI for different layers at a given elevation (tolerance is ± 3 ft) and zones are given in Figures 20 and 21, respectively. For Strata IIb-1, IIb-2, and IIb-3, the scatter in water content for a given zone can be as large as the overall scatter when all zones are considered. For Stratum IIb-1, Zone 1 has slightly higher water content than Zones 2, 3, 4 and 6. The value of water content for Zone 5 is relatively different when compared with other zones for Stratum IIb-1. For Stratum IIb-3, Zone 4 has slightly larger water content than Zone 2. Scatter in PI shown in Figure 21 is large and random.

Although a scatter was observed from the soil parameters studied in this calculation, there is no consistent trend correlating the variation of soil properties to specific footprint location. The potential impact of this variation on the settlement may be examined by establishing lower bounds for relevant soil parameters and conducting the settlement analysis with such lower-bound parameters.

Lower Bounds for Soil Parameters

The soil parameters used in calculation of the total settlement are unit weight, friction angle, apparent cohesion, dilation angle, Poisson's ratio and stiffness. Among these, the most influential soil parameter on settlement estimate is the soil stiffness.

Any of the following three approaches may be implemented to establish the lower bound parameters:

Approach 1 – Statistical Analysis

Statistical analysis was conducted on results from field testing or laboratory testing. Statistical analysis consisted of fitting a log-normal distribution to the data. A log-normal distribution with parameters ζ and λ is used in to represent the observed data. The log-normal distribution is considered to have a better "fit" to the observed data than the standard normal distribution, as this is verified using the Kolmogorov-Smirnov (K-S) "goodness of fit" test and observing the dispersion of data. The basic premise of the K-S test is to compare the experimental cumulative frequency with cumulative distribution function of log-normal distribution. The predictions are acceptable if the difference between experimental and theoretical distribution is less than a threshold determined based on a five percent significance level.

Approach 2 – Data Sorting Analysis

If the log-normal distribution suggested in Approach 1 does not fit to the data and there are enough data points, a different approach is required. Data is sorted from smallest to the largest, and a bounding value, above which 84 percent of the entire data set exists, is established. This value is close to the 16th percentile obtained from the statistical tests.

Approach 3 – Minimum Values based on Engineering Judgment

If neither Approach 1 nor Approach 2 is possible, i.e., there are not enough measurements in the power block area, a reasonable minimum value for the entire site is established as the lower bound.

An example of the methodology is provided for the statistical analysis on shear wave velocity tests results for Stratum IIb-1. A lower bound for the parameter estimate is considered to be the 16th percentile obtained from statistical tests, which corresponds to the average value minus standard deviation, in the logarithmic domain. Table 6 provides the shear wave velocity measurements for Stratum IIb-1. Table 7 and Figure 22 provide the comparison of the predicted (theoretical) and observed distributions of shear wave velocity data in the Powerblock area for Stratum IIb-1. Table 8 presents the calculated parameters and suggested lower bound (16th percentile).

The soil stiffness was obtained using results from P-S Suspension (through shear wave velocity), pressuremeter, dilatometer, SPT, undrained shear strength, and consolidation test results. Results from each test were analyzed and a lower bound was established from each test result. Then, the resultant lower bound stiffness was obtained by averaging the lower bound from each test. This approach is assumed to consider the variation involved in each test, giving a reasonable lower bound of stiffness.

The lower bound stiffness E as obtained from each test is provided in Table 9 along with information about which approach is used for results from each test. Table 9 also includes unload/reload stiffness E_R , which was determined based on E_R/E ratios given for each layer as shown in Table 9. Using a lower bound E and the best estimate E_R/E ratio is considered as the lower bound for E_R .

The lower bounds for the soil parameters are given in Table 10. For comparison purpose, the best estimate parameters are given in Table 11.

The data available for shear parameters of each layer is limited in the Powerblock area. Therefore, a reasonable lower bound was established using the minimum values from the entire site (Approach 3). No laboratory tests are available for the shear strength of Nanjemoy sand layer. The lower bounds for effective friction angle and apparent cohesion are conservatively assumed to be 30° and 0 tsf, respectively. The effective apparent cohesion term is difficult to estimate with very limited data. The minimum of zero effective apparent cohesion observed in limited number of tests is not a realistic lower bound, since the sands encountered on site have considerable amount of fines. Therefore, instead of assuming a zero cohesion, the effective apparent cohesion is assumed to be half of the best estimate numbers for all layers. The minimum effective friction angle for Stratum IIc was 19°, which is considered to be very low given the high E (Table 10 and Table 11) and

overconsolidation ratio (OCR) of 4. The lower-bound effective friction angle for this layer is assumed to be 25° , 7° less than the best estimate value.

The lower bound for the unit weight was determined based on the 16th percentile (Approach 1).

The lower bound of the dilation angle was assumed to be zero for all layers.

Expected variation in Poisson's ratio is not significant, and lower bound could be assumed to be the same as the best estimate.

Permeabilities were obtained based on calibration of the groundwater model with field tests. Furthermore, the permeability is not anticipated to impact the total settlement, but is expected to influence the settlement rate. Since this study aims to develop lower bounds for long term static settlement, the lower bound for permeability is assumed to be the same as the best estimate value.

The details of the statistical analysis conducted are given in Table 12.

Impact of Lower Bounds on Settlement

The MT2 model was considered as the best estimate case which was based on parameters given in Table 11 (best estimate parameters). This model was reevaluated using the parameters given in Table 10 to determine the effect of lower bound parameters on settlement. The resulting settlements for the center of all buildings in the power block area are given in Table 13. Also included in Table 13 are the resultant settlements observed from MT2 model with the best estimate parameters. As expected, the lower-bound parameters increase the predicted settlement. The increase in the settlement of reactor building is from 12.7 inches to 20.0 inches, while the highest settlement of 20.4 inches is predicted for the fuel building. Resultant construction-sequence-corrected tilt for both best estimate and lower bound cases are given in Table 14. Using lower-bound parameters increases the estimated tilt, as well. However, the increase in tilt for the nuclear island is not significant.

As expected, the lower-bound parameters result in larger settlements and tilts. For the settlement analysis, the properties that significantly impact the outcome are the soil modulus E and unit weight. The likelihood of having a lower bound E or unit weight for a given layer is low. In other words, about 84% of all measurements are higher than the lower bound value. The probability of having lower bound of E and unit weight for all soil layers at the same time would be much lower, very close to zero. The results obtained from the simultaneous use of the lower bound soil properties for every soil layer would represent an overconservative and unrealistic approach.

Table 6
V_s Data For Stratum IIb-1 in Powerblock Area

Sample		V _s	V _s
Depth	Elevation		
(ft)	(ft)	ft/s	ln(x)
52.5	42	1600.00	7.38
54.1	40.4	1920.00	7.56
55.8	38.7	2190.00	7.69
57.4	37.1	2060.00	7.63
59.1	35.4	1780.00	7.48
60.7	33.8	1610.00	7.38
62.3	32.2	1620.00	7.39
64	30.5	1590.00	7.37
65.6	28.9	1490.00	7.31
67.3	27.2	1700.00	7.44
68.9	25.6	1630.00	7.40
70.5	24	1690.00	7.43
72.2	22.3	3580.00	8.18
73.8	20.7	3370.00	8.12
75.5	19	3000.00	8.01
77.1	17.4	3550.00	8.17
78.7	15.8	3300.00	8.10
80.4	14.1	3250.00	8.09
82	12.5	2480.00	7.82
27.9	40.1	1550.00	7.35
29.5	38.5	1570.00	7.36
31.2	36.8	1680.00	7.43
32.8	35.2	1670.00	7.42
34.5	33.5	1780.00	7.48
36.1	31.9	1770.00	7.48
37.7	30.3	1630.00	7.40
39.4	28.6	1560.00	7.35
41	27	1560.00	7.35

Table 6 (cont)
V_s Data For Stratum IIb-1 in Powerblock Area

42.7	25.3	1530.00	7.33
44.3	23.7	1550.00	7.35
45.9	22.1	1880.00	7.54
47.6	20.4	2170.00	7.68
49.2	18.8	2320.00	7.75
50.9	17.1	2360.00	7.77
52.5	15.5	2960.00	7.99
54.1	13.9	2720.00	7.91
55.8	12.2	1710.00	7.44
27.9	40.1	1570.00	7.36
29.5	38.5	1690.00	7.43
31.2	36.8	1630.00	7.40
32.8	35.2	1560.00	7.35
34.5	33.5	1660.00	7.41
36.1	31.9	1780.00	7.48
37.7	30.3	1590.00	7.37
39.4	28.6	1490.00	7.31
41	27	1670.00	7.42
42.7	25.3	1600.00	7.38
44.3	23.7	1570.00	7.36
45.9	22.1	2010.00	7.61
47.6	20.4	2160.00	7.68
49.2	18.8	2040.00	7.62
50.9	17.1	2680.00	7.89
52.5	15.5	3020.00	8.01
54.1	13.9	2840.00	7.95
55.8	12.2	1920.00	7.56
73.8	45.5	1270.00	7.15
75.5	43.8	1520.00	7.33
77.1	42.2	2110.00	7.65
78.7	40.6	2530.00	7.84

Table 6 (cont)
V_s Data For Stratum IIb-1 in Powerblock Area

80.4	38.9	1800.00	7.50
82	37.3	1330.00	7.19
83.7	35.6	1400.00	7.24
85.3	34	1690.00	7.43
86.9	32.4	1880.00	7.54
88.6	30.7	2120.00	7.66
90.2	29.1	2000.00	7.60
91.9	27.4	1970.00	7.59
93.5	25.8	1940.00	7.57
95.1	24.2	1920.00	7.56
96.8	22.5	2410.00	7.79
98.4	20.9	3000.00	8.01
100.1	19.2	3320.00	8.11
101.7	17.6	3190.00	8.07
103.4	15.9	2080.00	7.64
55.8	42	1820.00	7.51
57.4	40.4	2210.00	7.70
59.1	38.7	1930.00	7.57
60.7	37.1	1820.00	7.51
62.3	35.5	1770.00	7.48
64	33.8	1570.00	7.36
65.6	32.2	1670.00	7.42
67.3	30.5	2020.00	7.61
68.9	28.9	1500.00	7.31
70.5	27.3	1550.00	7.35
72.2	25.6	1610.00	7.38
73.8	24	2040.00	7.62
75.5	22.3	2280.00	7.73
77.1	20.7	2420.00	7.79
78.7	19.1	2080.00	7.64
80.4	17.4	1760.00	7.47

Table 6 (cont)
V_s Data For Stratum IIb-1 in Powerblock Area

68.9	38.6	1390.00	7.24
70.5	37	1630.00	7.40
72.2	35.3	2420.00	7.79
73.8	33.7	2540.00	7.84
75.5	32	2030.00	7.62
77.1	30.4	1770.00	7.48
78.7	28.8	1440.00	7.27
80.4	27.1	1220.00	7.11
82	25.5	1160.00	7.06
83.7	23.8	1330.00	7.19
85.3	22.2	1170.00	7.06
86.9	20.6	1150.00	7.05
88.6	18.9	1190.00	7.08
90.2	17.3	1380.00	7.23
91.9	15.6	1790.00	7.49
93.5	14	2150.00	7.67
95.1	12.4	2140.00	7.67
96.8	10.7	1630.00	7.40

Table 7
V_s Predicted (Theoretical) and Observed Distributions for Powerblock Area

Interval ft/s	From Observed Data			Log-Normal Distribution			Difference
	Freq ⁽¹⁾	Cumul. Freq ⁽²⁾	Cumul. Prob ⁽³⁾	Cumul Prob ⁽³⁾	Freq ⁽¹⁾	Cumul Freq ⁽²⁾	Observed / Theoretical
< 1	0	0	0.000	0.000	0.0	0.0	0.00
1-50	0	0	0.000	0.000	0.0	0.0	0.00
50-100	0	0	0.000	0.000	0.0	0.0	0.00
100-150	0	0	0.000	0.000	0.0	0.0	0.00
150-200	0	0	0.000	0.000	0.0	0.0	0.00
200-250	0	0	0.000	0.000	0.0	0.0	0.00
250-300	0	0	0.000	0.000	0.0	0.0	0.00
300-350	0	0	0.000	0.000	0.0	0.0	0.00
350-400	0	0	0.000	0.000	0.0	0.0	0.00
400-450	0	0	0.000	0.000	0.0	0.0	0.00
450-500	0	0	0.000	0.000	0.0	0.0	0.00
500-550	0	0	0.000	0.000	0.0	0.0	0.00
550-600	0	0	0.000	0.000	0.0	0.0	0.00
600-650	0	0	0.000	0.000	0.0	0.0	0.00
650-700	0	0	0.000	0.000	0.0	0.0	0.00
700-750	0	0	0.000	0.000	0.0	0.0	0.000
750-800	0	0	0.000	0.001	0.0	0.1	0.001
800-850	0	0	0.000	0.001	0.1	0.1	0.001
850-900	0	0	0.000	0.002	0.1	0.3	0.002
900-950	0	0	0.000	0.004	0.2	0.5	0.004
950-1000	0	0	0.000	0.008	0.4	0.8	0.008
1000-1050	0	0	0.000	0.013	0.5	1.4	0.013
1050-1100	0	0	0.000	0.020	0.8	2.1	0.020
1100-1150	1	1	0.009	0.030	1.1	3.2	0.020
1150-1200	3	4	0.037	0.042	1.4	4.6	0.005
1200-1250	1	5	0.046	0.058	1.7	6.3	0.012
1250-1300	1	6	0.056	0.078	2.1	8.4	0.023
1300-1350	2	8	0.074	0.101	2.5	10.9	0.027
1350-1400	3	11	0.102	0.128	2.9	13.8	0.026
1400-1450	1	12	0.111	0.158	3.3	17.1	0.047
1450-1500	3	15	0.139	0.192	3.6	20.7	0.053
1500-1550	5	20	0.185	0.228	3.9	24.6	0.043
1550-1600	11	31	0.287	0.266	4.1	28.7	0.021

Table 7 (cont)
V_s Predicted (Theoretical) and Observed Distributions for Powerblock Area

1600-1650	8	39	0.361	0.306	4.3	33.0	0.055
1650-1700	9	48	0.444	0.347	4.4	37.5	0.097
1700-1750	1	49	0.454	0.389	4.5	42.0	0.065
1750-1800	9	58	0.537	0.430	4.5	46.5	0.107
1800-1850	2	60	0.556	0.472	4.5	51.0	0.084
1850-1900	2	62	0.574	0.513	4.4	55.4	0.062
1900-1950	5	67	0.620	0.552	4.3	59.6	0.068
1950-2000	2	69	0.639	0.590	4.1	63.7	0.049
2000-2050	5	74	0.685	0.626	3.9	67.6	0.059
2050-2100	3	77	0.713	0.660	3.7	71.3	0.053
2100-2150	4	81	0.750	0.693	3.5	74.8	0.057
2150-2200	3	84	0.778	0.723	3.3	78.1	0.055
2200-2250	1	85	0.787	0.751	3.0	81.1	0.036
2250-2300	1	86	0.796	0.777	2.8	83.9	0.020
2300-2350	1	87	0.806	0.800	2.6	86.4	0.005
2350-2400	1	88	0.815	0.822	2.3	88.8	0.007
2400-2450	3	91	0.843	0.842	2.1	90.9	0.001
2450-2500	1	92	0.852	0.860	1.9	92.9	0.008
2500-2550	2	94	0.870	0.876	1.7	94.6	0.006
2550-2600	0	94	0.870	0.891	1.6	96.2	0.020
2600-2650	0	94	0.870	0.904	1.4	97.6	0.033
2650-2700	1	95	0.880	0.915	1.3	98.8	0.036
2700-2750	1	96	0.889	0.926	1.1	100.0	0.037
2750-2800	0	96	0.889	0.935	1.0	101.0	0.046
2800-2850	1	97	0.898	0.943	0.9	101.8	0.045
2850-2900	0	97	0.898	0.950	0.8	102.6	0.052
2900-2950	0	97	0.898	0.957	0.7	103.3	0.058
2950-3000	3	100	0.926	0.962	0.6	103.9	0.036
3000-3050	1	101	0.935	0.967	0.5	104.4	0.032
3050-3100	0	101	0.935	0.971	0.5	104.9	0.036
3100-3150	0	101	0.935	0.975	0.4	105.3	0.040
3150-3200	1	102	0.944	0.978	0.4	105.7	0.034
3200-3250	1	103	0.954	0.981	0.3	106.0	0.028
3250-3300	1	104	0.963	0.984	0.3	106.3	0.021
3300-3350	1	105	0.972	0.986	0.2	106.5	0.014
3350-3400	1	106	0.981	0.988	0.2	106.7	0.006

Table 7 (cont)
V_s Predicted (Theoretical) and Observed Distributions for Powerblock Area

3400-3450	0	106	0.981	0.990	0.2	106.9	0.008
3450-3500	0	106	0.981	0.991	0.2	107.0	0.009
3500-3550	1	107	0.991	0.992	0.1	107.2	0.001
3550-3600	1	108	1.000	0.993	0.1	107.3	0.007
3600-3650	0	108	1.000	0.994	0.1	107.4	0.006
3650-3700	0	108	1.000	0.995	0.1	107.5	0.005
3700-3750	0	108	1.000	0.996	0.1	107.5	0.004
3750-3800	0	108	1.000	0.996	0.1	107.6	0.004
3800-3850	0	108	1.000	0.997	0.1	107.7	0.003
3850-3900	0	108	1.000	0.997	0.0	107.7	0.003
3900-3950	0	108	1.000	0.998	0.0	107.7	0.002
3950-4000	0	108	1.000	0.998	0.0	107.8	0.002

(1) Freq = Frequency

(2) Cumu. Freq. = Cumulative Frequency

(3) Cumu. Prob. = Cumulative Probability

Table 8
Calculation of Lower Bound Shear Wave Velocity

PARAMETER	VALUE	NOTES
Total data points	108	
Minimum value	0	
Maximum value	3580	
Average	1953.0	Arithmetic mean
Standard Deviation	557.1	
Average minus Standard Deviation	1395.8	
Average (Ln(x))	7.541	Parameter ζ of the log-normal
Standard Deviation (Ln(x))	0.262	Parameter λ of the log-normal
Avg(Ln(x)) - Stdev(Ln(x))	7.280	
16 Percentile	1450.4	$\exp[\text{Avg}(\text{Ln}(x)) - \text{Stdev}(\text{Ln}(x))]$
K-S D_{\max}	0.11	Maximum difference between the observed and theoretical frequencies
K-S α	5%	Significance value for the test
K-S $D_{n,\alpha}$	0.13	Critical difference
$D_{\max} < D_{n,\alpha}$	✓	Acceptable fit

Table 9
Lower Bound for Primary Stiffness E and Unloading/Reloading Stiffness E_r

LAYER	Geophysical	Pressuremeter	Dilatometer	SPT		S _u		Consolidation	Arithmetic Mean E	Standard Deviation E	E _R
				E = 18N ₆₀	E = b ₀ √OCR + b ₁ N ₆₀	E = 450s _u	E = 2*G _{stat} (1+n)		psf	psf	
Layer Iib - 1	1.89E+06	1.24E+06	7.13E+06	9.96E+05	4.90E+05				2.35E+06	2.72E+06	7.05E+06
Layer Iib - 2	8.32E+05	9.26E+05	1.37E+06	4.98E+05	2.53E+05				7.75E+05	4.26E+05	3.46E+06
Layer Iib - 3	2.91E+06	1.85E+06	2.18E+06	1.06E+06	5.11E+05				1.70E+06	9.40E+05	6.62E+06
Layer Iic	1.22E+06	1.22E+06	7.41E+05			1.60E+06	2.03E+06	1.21E+06	1.34E+06	4.37E+05	4.01E+06
Nanjemoy	3.18E+06	1.96E+06	8.12E+05	1.83E+06	6.81E+05				1.69E+06	1.01E+06	5.18E+06

Table 10
Lower Bound for Soil Parameters

LAYER	Unit Weight	Apparent Cohesion, c'	Friction Angle, ϕ'	E_r	E	Dilation Angle	Poisson's Ratio, ν'
	pcf	psf	degrees	psf	psf	degrees	
IIb - Chesapeake Cemented Sand (1)	111	300	26	4.57E+06	1.52E+06	0	0.30
IIb - Chesapeake Cemented Sand (2)	111	260	27	2.98E+06	6.67E+05	0	0.30
IIb - Chesapeake Cemented Sand (3)	117	110	28	5.63E+06	1.45E+06	0	0.30
IIc - Chesapeake Clay/Silt	96	400	25	3.83E+06	1.28E+06	0	0.35
IIc - Chesapeake Clay/Silt - Sand	96	400	25	3.83E+06	1.28E+06	0	0.30
II - Nanjemoy Sand	119	0	30	4.42E+06	1.45E+06	0	0.00

Table 11
Best Estimate Parameters

LAYER	Unit Weight	Apparent Cohesion, c'	Friction Angle, ϕ'	E_r	E	Dilation Angle	Poisson's ratio, ν'
	pcf	psf	degrees	psf	psf	degrees	
IIb - Chesapeake Cemented Sand (1)	122	600	34	7.59E+06	2.53E+06	0	0.30
IIb - Chesapeake Cemented Sand (2)	123	520	32	4.60E+06	1.03E+05	0	0.30
IIb - Chesapeake Cemented Sand (3)	123	220	32	1.02E+07	2.62E+06	0	0.30
IIc - Chesapeake Clay/Silt	104	800	32	7.11E+06	2.37E+06	0	0.35
IIc - Chesapeake Clay/Silt - Sand	104	800	32	7.11E+06	2.37E+06	0	0.30
II - Nanjemoy Sand	127	0	40	9.70E+06	3.17E+06	0	0.30

Table 12
Details of the Statistical Analysis

		$D_{max}^{(1)}$	$D_{n,\alpha}^{(2)}$	Degree of Freedom	K-S Test Result	Lower Bound	Unit	Lower Bound	Approach
Geophysical, Shear Wave Velocity	Layer IIb - 1	0.11	0.13	71	acceptable	1450	ft/s		Approach 1
	Layer IIb - 2	0.14	0.16	71	acceptable	965	ft/s		Approach 1
	Layer IIb - 3	0.06	0.22	40	acceptable	1752	ft/s		Approach 1
	Layer IIc	0.09	0.07	351	acceptable ⁽³⁾	1191	ft/s		Approach 1
	Nanjemoy	0.09	0.19	54	acceptable	1817	ft/s		Approach 1
Pressuremeter, E	Layer IIb - 1	0.17	0.56	6	acceptable	8613	psf		Approach 1
	Layer IIb - 2	0.30	0.56	6	acceptable	6432	psf		Approach 1
	Layer IIb - 3	0.30	0.68	4	acceptable	12830	psf		Approach 1
	Layer IIc	0.16	0.23	36	acceptable	8439	psf		Approach 1
	Nanjemoy	0.18	0.51	7	acceptable	13641	psf		Approach 1
Dilatometer, E	Layer IIb - 1	0.34	0.79	3	acceptable	49485	psf		Approach 1
	Layer IIb - 2	0.12	0.25	30	acceptable	9484	psf		Approach 1
	Layer IIb - 3	0.17	0.43	10	acceptable	15144	psf		Approach 1
	Layer IIc	0.06	0.08	287	acceptable	5144	psf		Approach 1
	Nanjemoy	0.08	0.17	66	acceptable	15144	psf		Approach 1
Unit Weight	Layer IIb - 1	0.13	0.39	12	acceptable	111	pcf		Approach 1
	Layer IIb - 2	0.23	0.48	8	acceptable	111	pcf		Approach 1
	Layer IIb - 3	0.08	0.48	8	acceptable	117	pcf		Approach 1
	Layer IIc	0.06	0.19	50	acceptable	96	pcf		Approach 1
	Nanjemoy	0.12	0.61	5	acceptable	119	pcf		Approach 1
SPT	Layer IIb - 1	0.21	0.07	359	not acceptable			28	Approach 2
	Layer IIb - 2	0.10	0.07	335	not acceptable			14	Approach 2
	Layer IIb - 3	0.12	0.10	197	acceptable ⁽³⁾	29	-		Approach 1
	Layer IIc	0.07	0.06	562	acceptable ⁽³⁾	21	-		Approach 1
	Nanjemoy	0.16	0.30	20	acceptable	51	-		Approach 1

⁽¹⁾ Maximum difference between the observed and theoretical frequencies

⁽²⁾ Critical difference

⁽³⁾ Since D_{max} and $D_{n,\alpha}$ are close and degree of freedom is large, the log-normal distribution is assumed to fit the data

Table 13
Comparison of Building Center Settlements, Best Estimate and Lower Bound MT2 Models

Building Name		Settlement (in)	
		Best Estimate	Lower Bound
Reactor Building	REACTOR	12.7	20.0
Fuel Building	FB	13.0	20.4
Safeguard Building 1	SGB1	12.0	20.2
Safeguard Building 2 and 3	SGB23	11.6	19.0
Safeguard Building 4	SGB4	12.5	19.5
Nuclear Auxiliary Building	NAB	12.3	19.2
Access Building	AB	11.7	18.8
Radioactive Waste Building	RWB	9.6	15.8
Emergency Service Water Building 1	ESWB1	7.4	11.9
Emergency Service Water Building 2	ESWB2	9.1	14.7
Emergency Service Water Building 3	ESWB3	9.2	14.8
Emergency Service Water Building 4	ESWB4	8.2	13.0
Emergency Power Generating Building 1	EPGB1	9.6	15.9
Emergency Power Generating Building 2	EPGB2	8.7	14.5

Table 14
Comparison of Tilts, Best Estimate and Lower Bound MT2 Models

Building Name	Section Label	Tilt (in / 50 ft)	
		Best Estimate	Lower Bound
Nuclear Island Common Mat	AA	0.10	0.15
	BB	0.27	0.28
	CC	0.21	0.39
	DD	0.32	0.39
Emergency Service Water Building 1	EE	0.59	1.02
	FF	0.18	0.29
Emergency Service Water Building 2	GG	0.23	0.42
	HH	0.72	1.26
Emergency Service Water Building 3	II	0.17	0.25
	JJ	0.13	0.27
Emergency Service Water Building 4	KK	0.28	0.45
	LL	0.42	0.69
Emergency Power Generating Building 1	MM	0.16	0.28
	NN	0.49	0.74
Emergency Power Generating Building 2	OO	0.42	0.80
	PP	0.14	0.28

Zones Selected for the Assessment of Soil Parameter Variability

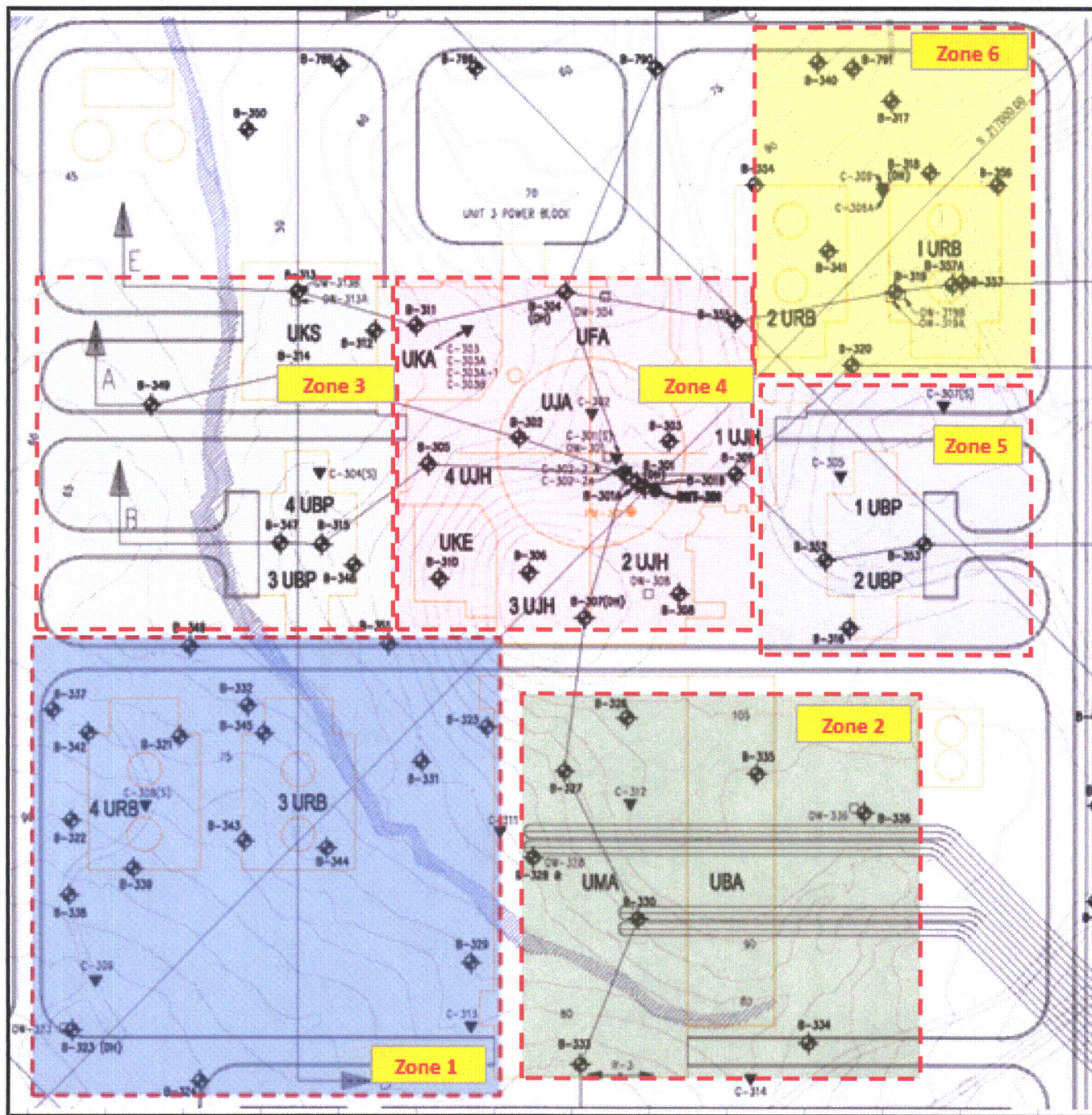


Figure 17
Shear Wave Velocity Distribution for Different Borings at Given Elevations

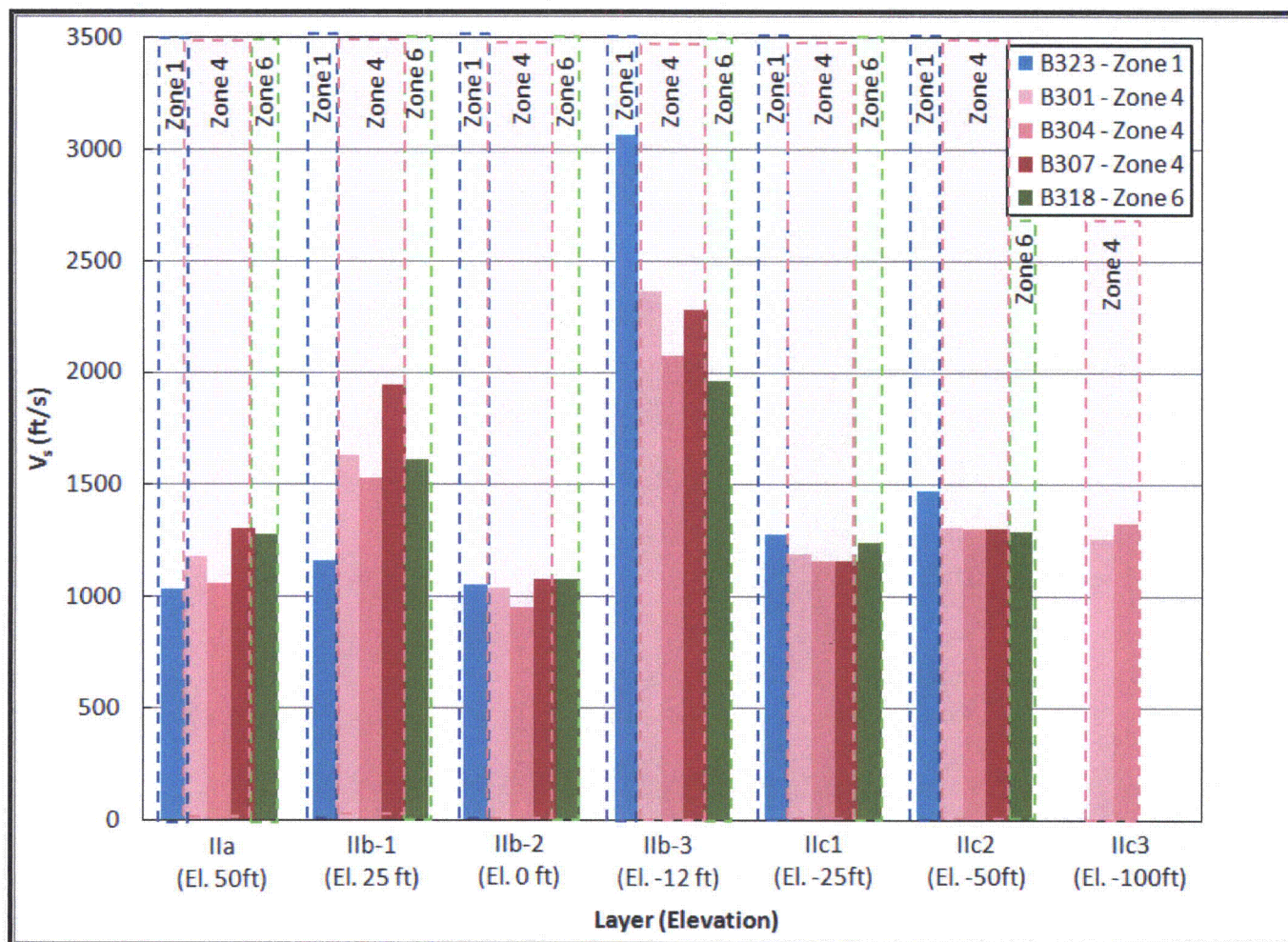


Figure 18
N₆₀ Distribution for Different Borings at Given Elevations

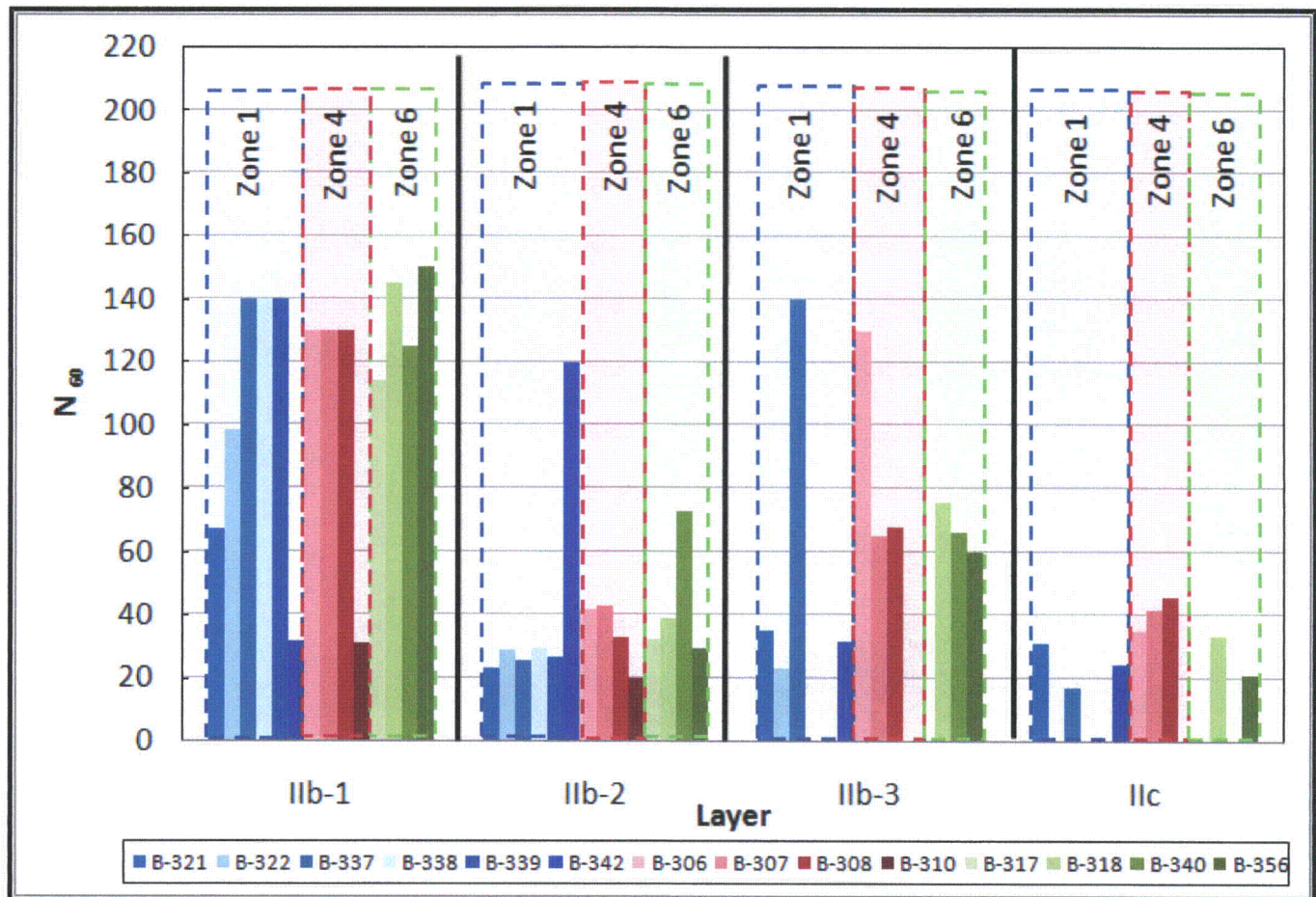


Figure 19
 N_{160} Distribution for Different Borings at Given Elevations

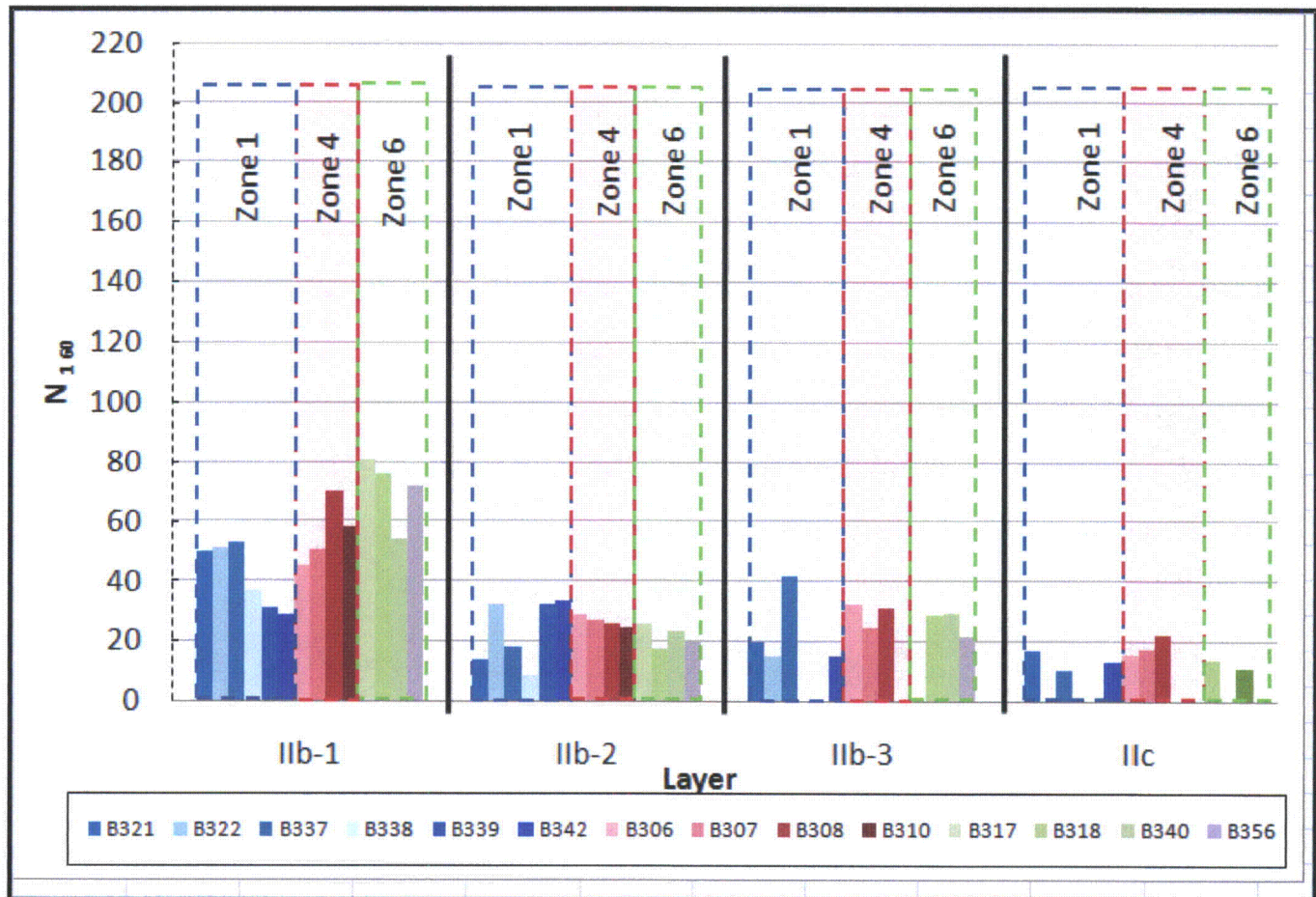


Figure 20
Water Content (W) Distribution for Different Borings at Given Elevations

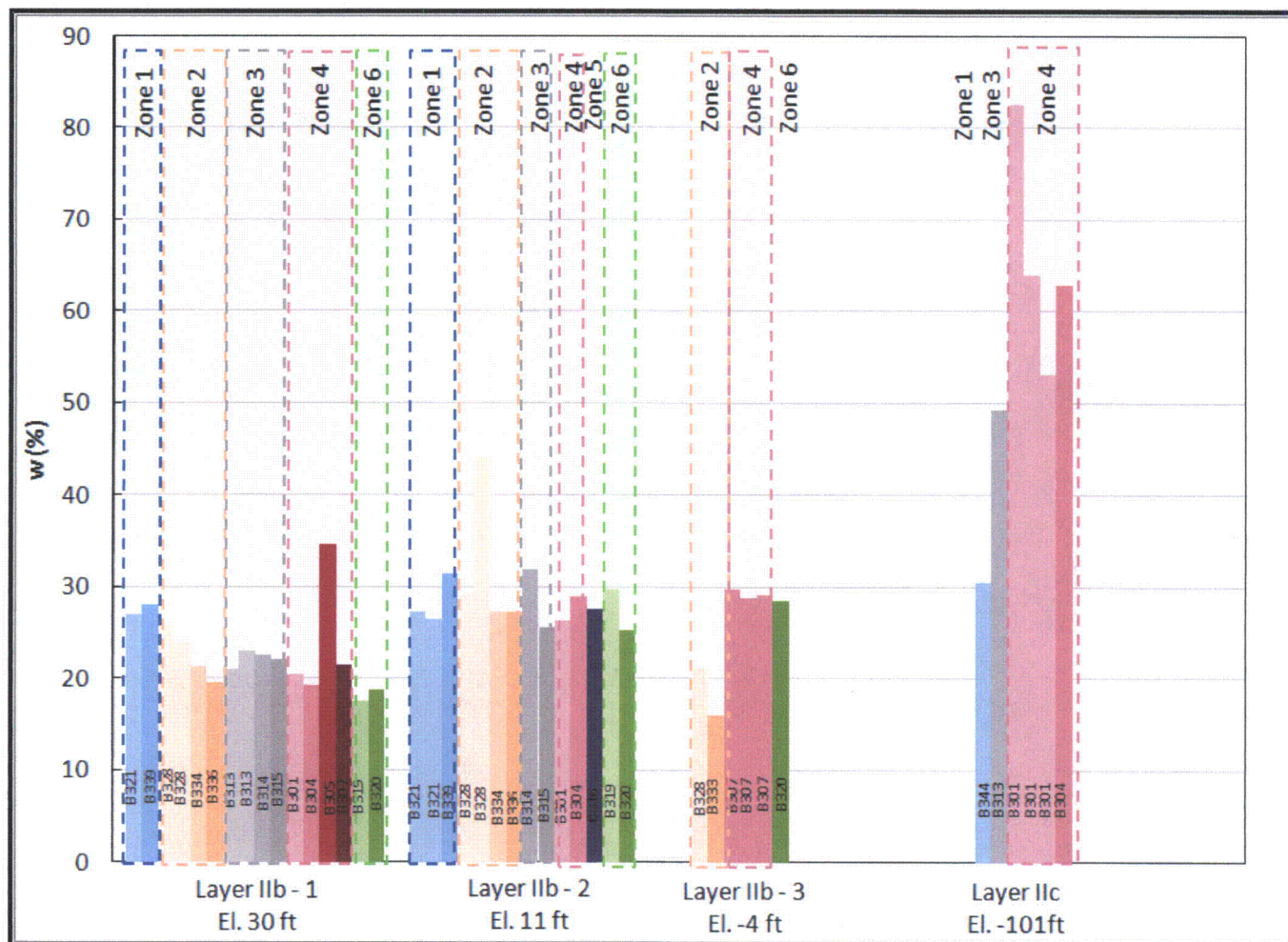


Figure 21
PI Distribution for Different Borings at Given Elevations

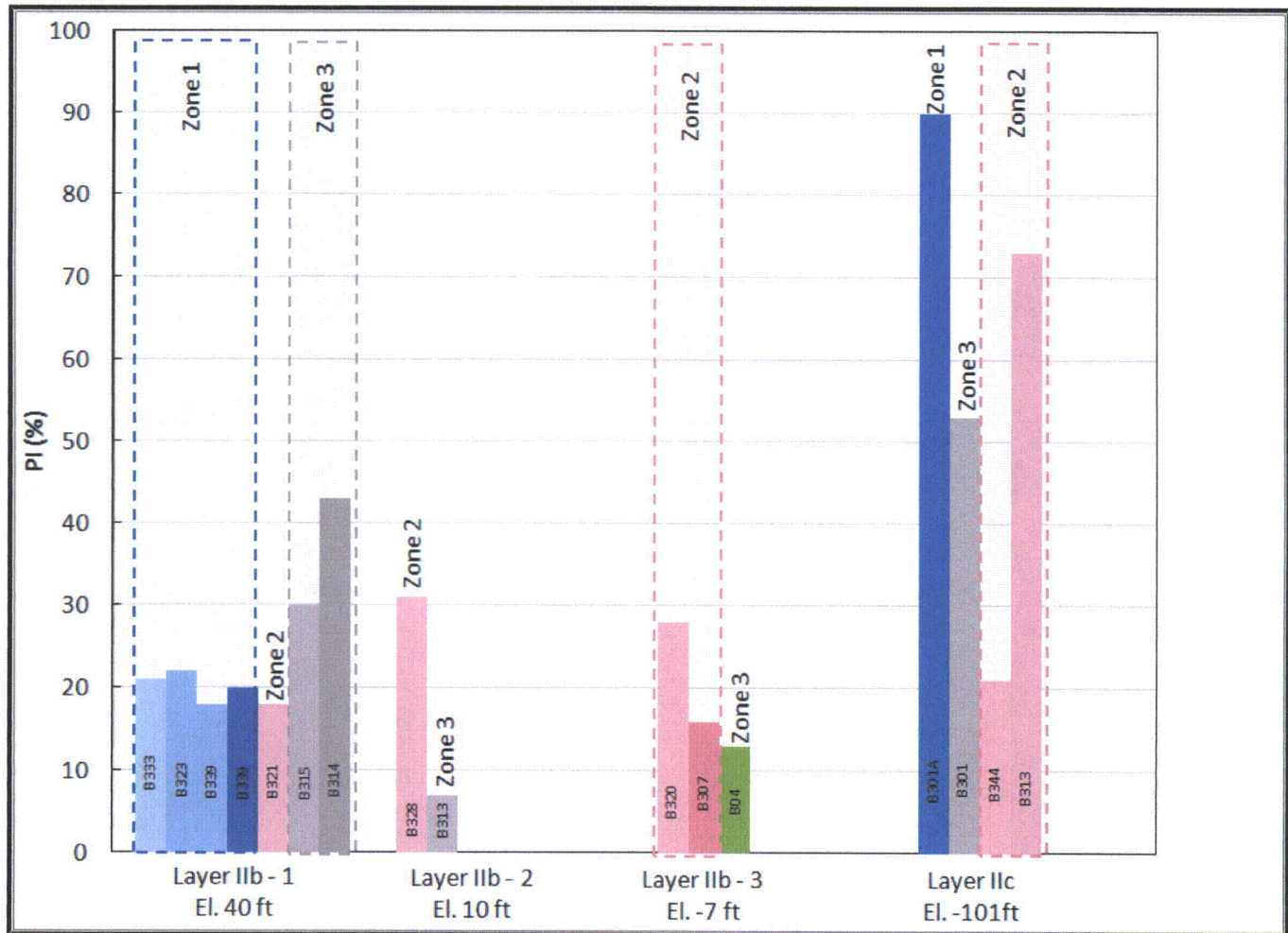
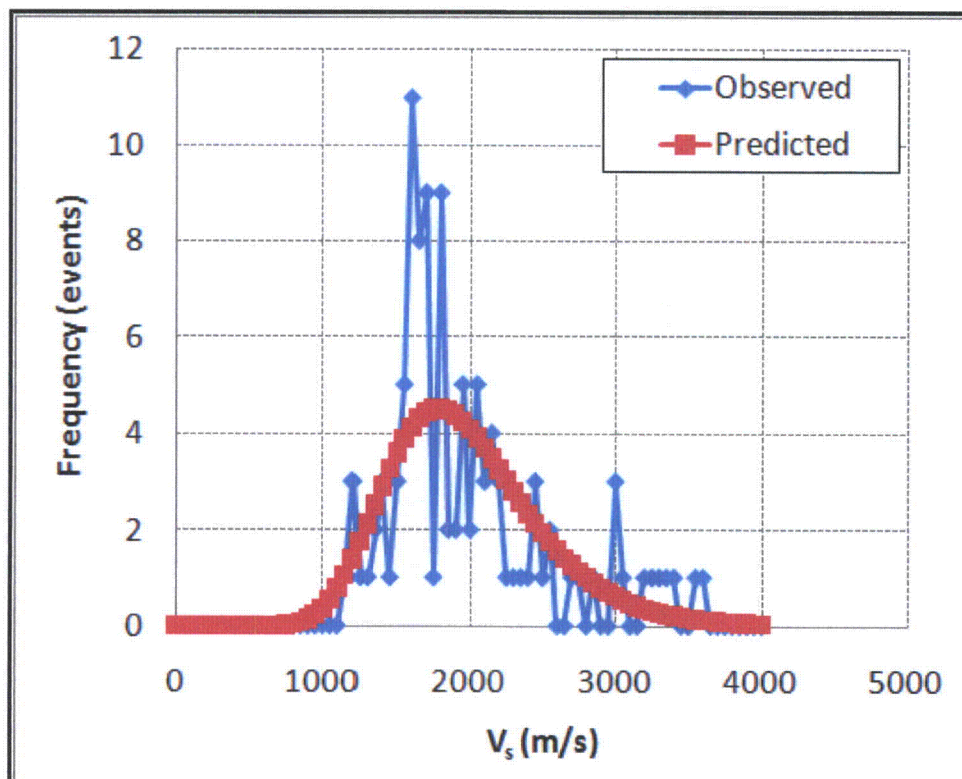


Figure 22
Histograms for the Observed and Predicted Shear Wave Velocities



Part 4:

Settlements (u_y) at the base of the building foundations are used to compute the differential settlements (Δu_y) between the NI and adjacent buildings using the MT2 model results.

Differential settlements between the NI and each adjacent building are determined for pairs of points at the center of the NI and each surrounding building, and also for pairs of points at the edges of the NI and each surrounding building. For the edge to edge case, the closest points for the selected building pairs are considered. Also considered is the differential settlement between RWPB and NAB.

While calculating the differential settlement, the effect of the construction sequence is considered. The output from the MT2 model consists of settlements at the end of each of 8 loading steps. The construction sequence indicates that construction of different buildings starts at different loading steps. For example, EPGB construction starts at the 6th loading step, and any deformation obtained from the model prior to 6th loading step should be subtracted from the total deformation obtained at the end of 8th loading step. This correction aims to address the fact that construction for each building is expected to start on a level ground.

Differential settlements (Δu_y) for the pairs were computed by using the definition below:

$$\Delta u_y = (u_y)_{\text{Adj. Bldg.}} - (u_y)_{\text{NI}}$$

where $(u_y)_{\text{Adj. Bldg.}}$ and $(u_y)_{\text{NI}}$ are the settlements at the end of 8th loading step and at the base of the adjacent building and NI, respectively.

The settlements and resulting differential settlements are tabulated in Table 15. Figure 23 shows the location of points considered for differential settlements.

The U.S. EPR standard design does not include specific requirements for the differential settlements between buildings. As shown in Table 15, the largest inter-building differential settlement was close to 9.8 inches between the center of the NI and the center of EPGB2. This difference will be minimized by the time interval in construction, much of the NI settlement will have occurred prior to connection being made between the buildings. The side-by-side Seismic Category I Buildings have edge-to-edge differential settlements of less than an inch. Thus, differential settlements expected between Cat I buildings do not pose a construction concern.

Table 15
Building Points with Associated Differential Settlements

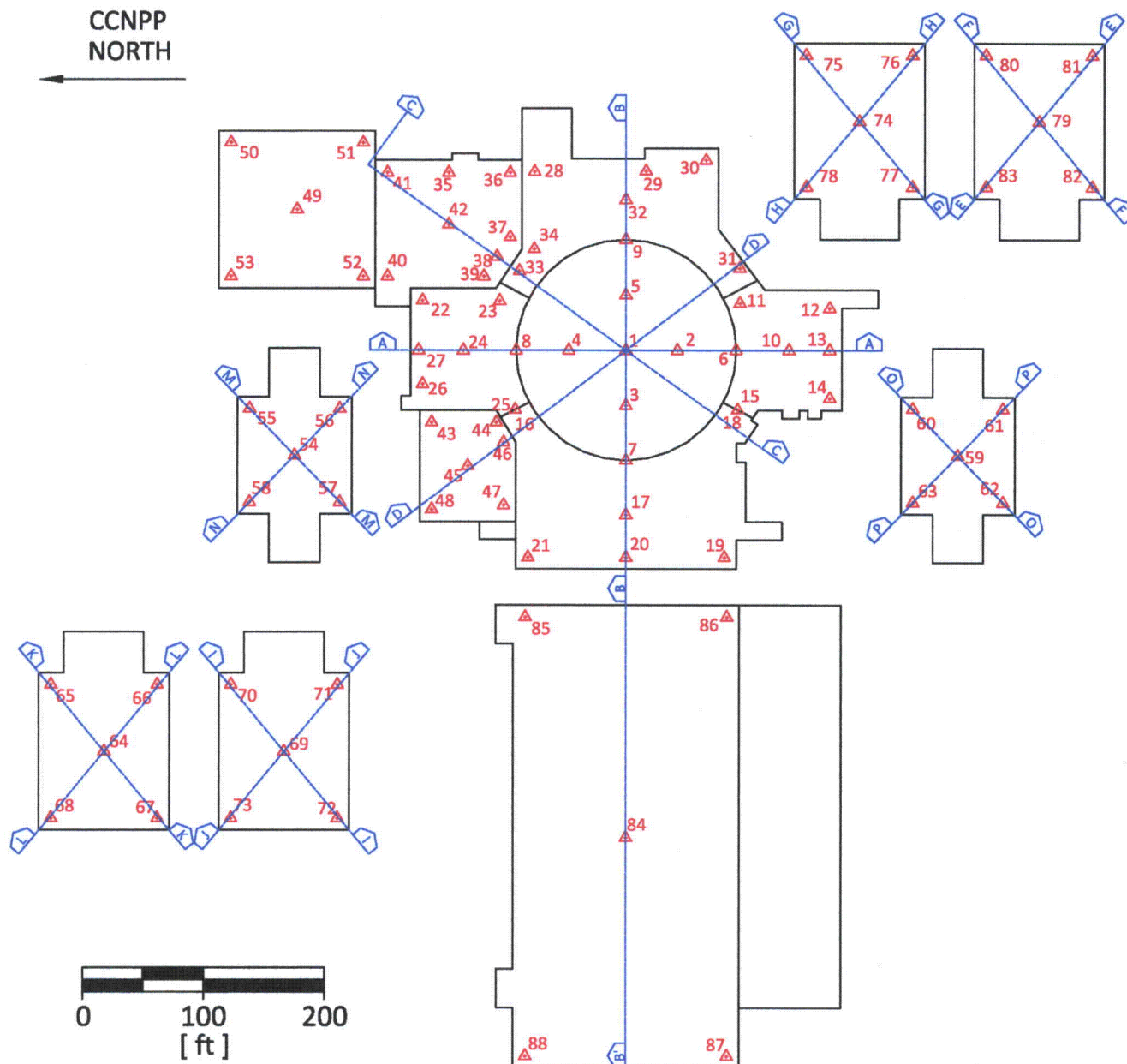
Building Name		Pair of Point No.		u _y (in.)		Δu _y (in.)
		NI	Adj. Bldg.	NI	Adj. Bldg.	
Emergency Power Generating Building 1 (EPBG1)	Center	1	54	12.7	3.7	9.1
	Edge	21	57	10.7	3.9	6.8
	Edge	22	56	12.1	4.4	7.7
	Edge	26	56	11.6	4.4	7.2
Emergency Power Generating Building 2 (EPBG2)	Center	1	59	12.7	3.0	9.8
	Edge	12	60	11.4	3.5	7.8
	Edge	14	60	10.9	3.5	7.4
	Edge	19	63	10.4	3.1	7.2
Emergency Service Water Building 2 (ESWB2)	Center	1	74	12.7	6.2	6.6
	Edge	12	77	11.4	6.5	4.8
	Edge	12	78	11.4	7.4	3.9
	Edge	30	75	12.4	5.8	6.6
	Edge	30	78	12.4	7.4	4.9
	Edge	31	77	12.3	6.5	5.7
	Edge	31	78	12.3	7.4	4.8
Emergency Service Water Building 3 (ESWB3)	Center	1	69	12.7	5.9	6.8
	Edge	21	70	10.7	6.1	4.6
	Edge	21	71	10.7	6.1	4.6
	Edge	21	72	10.7	5.5	5.1
	Edge	26	70	11.6	6.1	5.4
	Edge	26	71	11.6	6.1	5.5
Turbine Building (TB)	Center	1	84	12.7	8.9	3.9
	Edge	19	86	10.4	10.3	0.0
	Edge	20	85	10.7	10.3	0.4
	Edge	20	86	10.7	10.3	0.3
	Edge	21	85	10.7	10.3	0.4
Nuclear Auxiliary Building (NAB)	Center	1	42	12.7	11.9	0.8
	Edge	22	40	12.1	11.4	0.7
	Edge	23	39	12.6	13.3	0.7
	Edge	28	36	12.3	12.3	0.0
	Edge	33	38	12.7	13.3	0.6
	Edge	34	37	12.7	13.3	0.6
	Edge	36	28	12.3	12.3	0.0
Access Building (AB)	Center	1	45	12.7	11.3	1.4
	Edge	16	46	12.1	12.3	0.2
	Edge	21	47	10.7	11.2	0.5
	Edge	25	44	12.1	12.6	0.4
	Edge	26	43	11.6	11.6	0.1
		RWPB	NAB	RWPB	NAB	
Radwaste Building (RWPB) - Nuclear Auxiliary Building (NAB)		51	41	7.3	10.1	2.7
		52	40	8.7	11.4	2.6

u_y (NI) - Settlements at the end of the 8th loading step at the base of the NI

u_y (Adj. Bldg)- Settlements at the end of the 8th loading step at the base of the adjacent building

Δu_y - Differential Settlements

Figure 23
Location Of Points Considered For Differential Settlements.



Part 5:

The main assumption used in the hand calculation is that the subsurface can be represented by sub-layers with elastic, homogenous and isotropic properties. The stress distribution used in the settlement calculation was calculated by induced stresses based on elastic theory. The induced stresses due to foundation loads were calculated to a predetermined depth, typically as twice the equivalent foundation width. This predetermined depth, as the zone of interest in the settlement calculation, was divided into 10 foot thick sub-layers and the settlement at each sub-layer was calculated using Boussinesq solution. Total elastic settlement was obtained by addition of the settlements from all sub-layers. Similarly, the consolidation settlements were calculated for each sub-layer by considering the induced stresses.

Both theory and experience have shown that the shape of the pressure bells (induced stress distribution) is more or less independent of the physical properties of the loaded subsurface. That is, the stress increase due to external loads is not a function of soil properties. Nevertheless, this assumption is not valid for subsurface materials with significant stiffness impedance. The difference between the stiffness of adjacent layers at CCNPP Unit 3 is not significant; therefore, it is valid to consider that the stress distribution is independent of the soil properties.

To further investigate the validation of the assumption for the CCNPP Unit 3 settlement calculation, a finite element numerical model was generated to replicate the subsurface conditions at boring log B-301. A numerical model was generated using PLAXIS two-dimensional (2D) finite element analysis software. The model includes a circular footing loaded uniformly with 5,930 psf. The layer thicknesses and soil properties considered in the model were based on boring B-301 (Table 16). The axisymmetric finite element model is shown in Figure 24. Fifteen node triangular elements were used with linear elastic material properties.

The Boussinesq equations used for induced stresses under circular loading is given as:

$$\sigma_z = p \left[1 - \left(\frac{1}{\left[1 + \left(\frac{r}{z} \right)^2 \right]^{3/2}} \right) \right]$$

where σ_z is the vertical stress p is the applied external pressure, r is the radius of external pressure (159.7 ft), and z is the depth of the vertical stresses of interest. A total depth of 800 ft was considered in the model.

The vertical stresses beneath the center of the foundation are presented in Figure 25 from finite element simulations and Boussinesq solutions. It is clear from the comparison of the two approaches that the difference between the theoretical solution without any stiffness input and a layered subsurface model is marginal. This finding indicates that the assumption, for the determination of stress increases in each layer, used in the hand calculation of settlement is valid and does not affect the settlement results.

Table 16
Soil Properties Used In Finite Element Model

Soil Layer	Model	Elastic Modulus E_{ref} [psf]	Poisson's Ratio	Thickness [ft]
IIb - 1	Linear Elastic	2.53E+06	0.3	29
IIb - 2	Linear Elastic	1.03E+06	0.3	20
IIb - 3	Linear Elastic	2.62E+06	0.3	10
IIc	Linear Elastic	2.37E+06	0.3	190
III	Linear Elastic	3.17E+06	0.3	551

Figure 24
Finite Element Model Used to Calculate Induced Stresses due to Foundation Loading

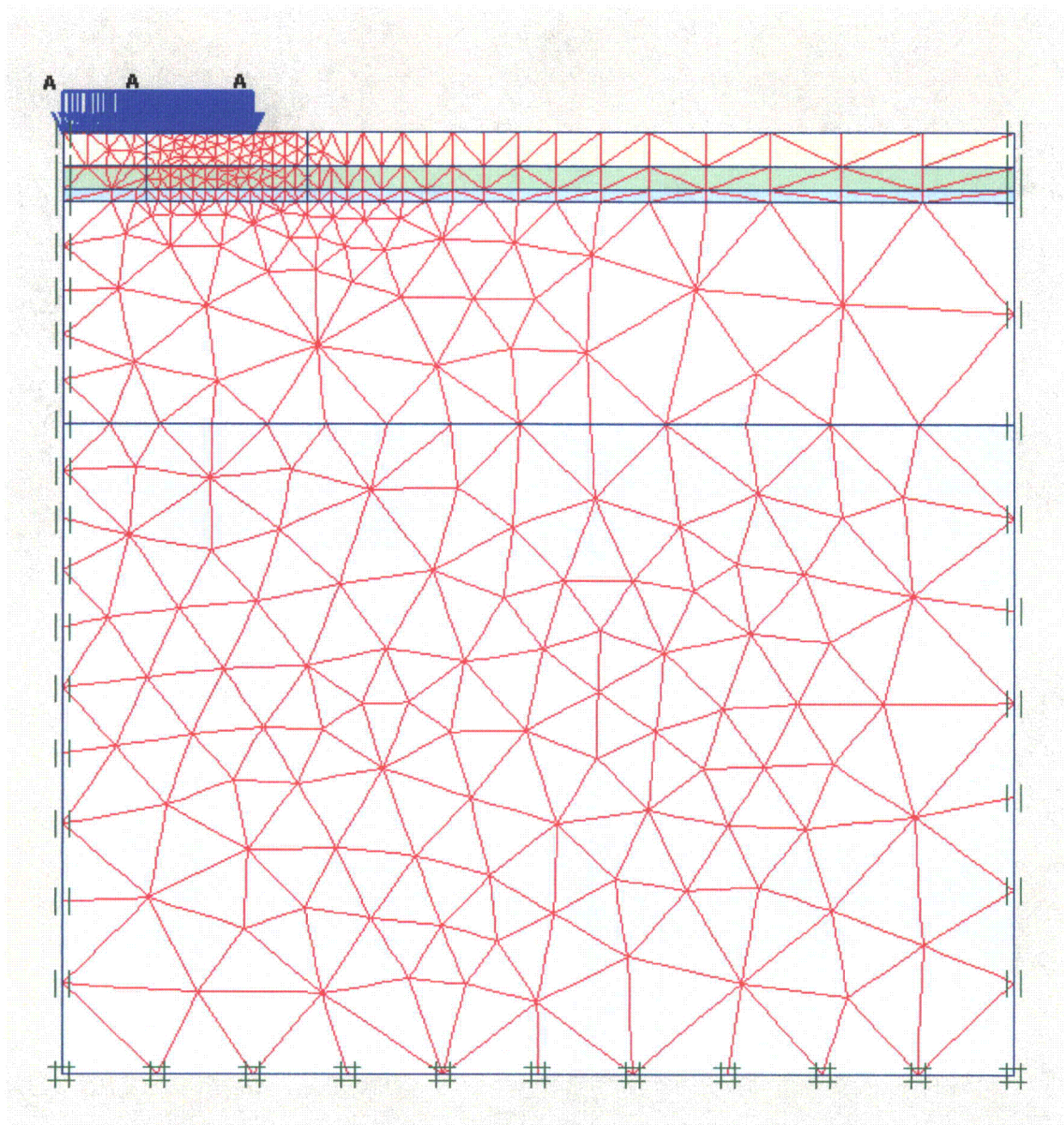
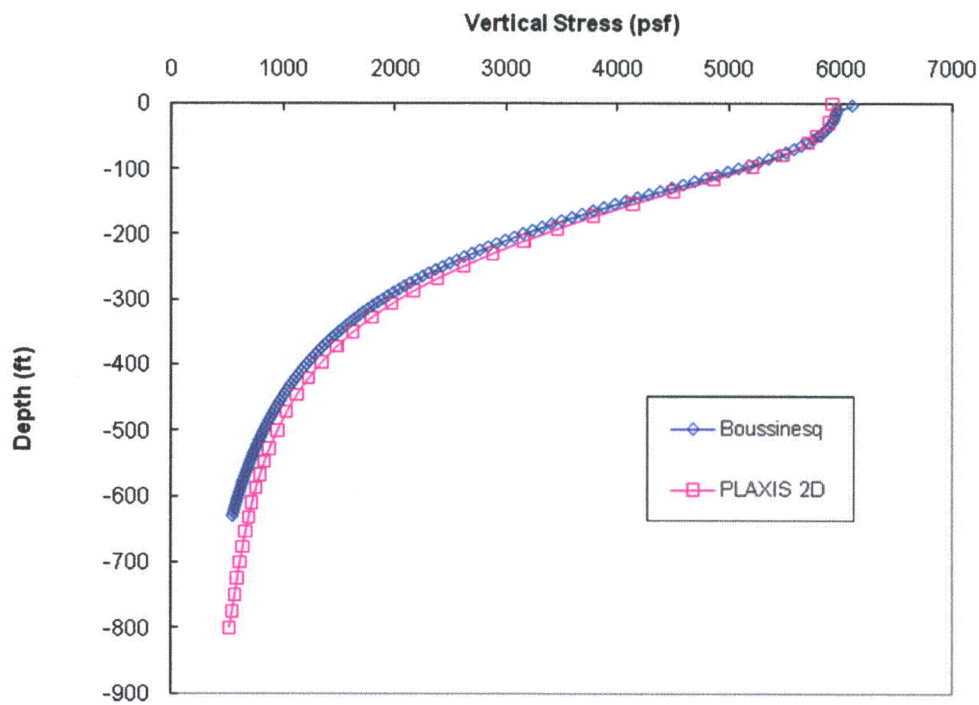


Figure 25
Vertical Stress Comparison



COLA Impact

Changes discussed in Part 2 and 3 of this response are incorporated into Section 2.5.4.10.2.2, and new Table 2.5-101 added. In addition Figure 2.5-194 is no longer required and is removed as shown below. Parts 1, 4 and 5 did not result in COLA changes.

2.5.4.10.2.2 Settlement and Heave Analysis in the CCNPP Powerblock Area

...

Settlement Analysis Results

...

- ◆ Figure 2.5-193 : Foundation base settlement for four sections of the NI and Turbine Building;

The figure indicates how the foundation settles after each step of the construction sequence. The results in the figure correspond to data resulting from the topography case that conservatively provides settlement at the centerline of the reactor ("Medium Elevation E Revert (2)").

- ◆ Table 2.5-101 presents differential settlements between the NI and adjacent buildings. The differential settlements are also shown in Table 2.5-101. Figure 2.5-192 shows the location of points considered for differential settlements.

Differential settlements between the NI and each adjacent building are determined for pairs of points at the center of the NI and each surrounding building, and also for pairs of points at the edges of the NI and each surrounding building. For the edge to edge case, the closest points for the selected building pairs are considered. Also considered is the differential settlement between RWPB and NAB.

While calculating the differential settlement, the effect of the construction sequence is considered. The output from the model consists of settlements at the end of each one of 8 loading steps. The construction sequence indicates that construction of different buildings start at different loading steps. For example, EPGB construction starts at the 6th loading step, and any deformation obtained from the model prior to 6th loading step should be subtracted from the total deformation obtained at the end of 8th loading step. This correction aims to address the fact that construction for each building is expected to start on a level ground.

Differential settlements (Δu_y) for the pairs were computed by using the definition below:

$$(\Delta u_y) = (u_y)_{Adj. Bldg.} - (u_y)_{NI}$$

where $(u_y)_{Adj. Bldg.}$ and $(u_y)_{NI}$ are the settlements at the end of 8th loading step and at the base of the adjacent building and NI, respectively.

The U.S. EPR standard design does not include specific requirements for the differential settlements between buildings. As shown in Table 2.5-101, the largest inter-building differential settlement was close to 9.8 inches between the center of the NI and the center of EPGB2. This difference will be minimized by the time interval in construction, much of the NI settlement will have occurred prior to connection being made between the buildings. The side-by-side Seismic Category I Buildings have edge-to-edge differential settlements of less than an inch. Thus, differential settlements expected between Cat I buildings do not pose a construction concern.

- ◆ Table 2.5-69: Maximum recorded tilt for the structures in the Powerblock Area.
- ◆ Figure 2.5-195: provides the settlement underneath each facility corresponding to the cases that analyze the sensitivity on surface topography. Low elevation points will have an increase in settlement after adjustment and high elevation points will see their settlement estimates reduced.

Table 2.5-101
Building Points with Associated Differential Settlements

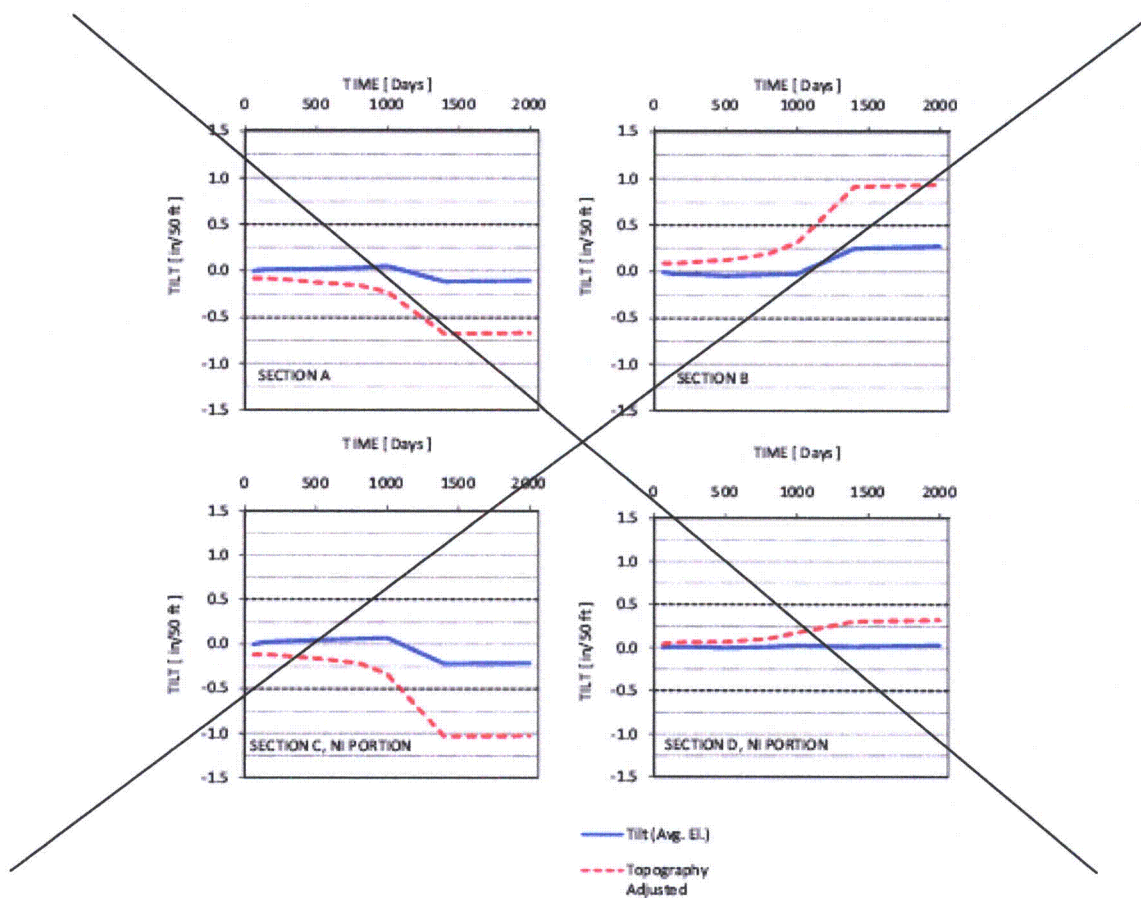
Building Name		Pair of Point No.		u_v (in.)		Δu_v (in.)
		NI	Adj. Bldg.	NI	Adj. Bldg.	
Emergency Power Generating Building 1 (EPBG1)	Center	1	54	12.7	3.7	9.1
	Edge	21	57	10.7	3.9	6.8
	Edge	22	56	12.1	4.4	7.7
	Edge	26	56	11.6	4.4	7.2
Emergency Power Generating Building 2 (EPBG2)	Center	1	59	12.7	3.0	9.8
	Edge	12	60	11.4	3.5	7.8
	Edge	14	60	10.9	3.5	7.4
	Edge	19	63	10.4	3.1	7.2
Emergency Service Water Building 2 (ESWB2)	Center	1	74	12.7	6.2	6.6
	Edge	12	77	11.4	6.5	4.8
	Edge	12	78	11.4	7.4	3.9
	Edge	30	75	12.4	5.8	6.6
	Edge	30	78	12.4	7.4	4.9
	Edge	31	77	12.3	6.5	5.7
	Edge	31	78	12.3	7.4	4.8
Emergency Service Water Building 3 (ESWB3)	Center	1	69	12.7	5.9	6.8
	Edge	21	70	10.7	6.1	4.6
	Edge	21	71	10.7	6.1	4.6
	Edge	21	72	10.7	5.5	5.1
	Edge	26	70	11.6	6.1	5.4
	Edge	26	71	11.6	6.1	5.5
Turbine Building (TB)	Center	1	84	12.7	8.9	3.9
	Edge	19	86	10.4	10.3	0.0
	Edge	20	85	10.7	10.3	0.4
	Edge	20	86	10.7	10.3	0.3
	Edge	21	85	10.7	10.3	0.4
Nuclear Auxiliary Building (NAB)	Center	1	42	12.7	11.9	0.8
	Edge	22	40	12.1	11.4	0.7
	Edge	23	39	12.6	13.3	0.7
	Edge	28	36	12.3	12.3	0.0
	Edge	33	38	12.7	13.3	0.6
	Edge	34	37	12.7	13.3	0.6
	Edge	36	28	12.3	12.3	0.0
Access Building (AB)	Center	1	45	12.7	11.3	1.4
	Edge	16	46	12.1	12.3	0.2
	Edge	21	47	10.7	11.2	0.5
	Edge	25	44	12.1	12.6	0.4
	Edge	26	43	11.6	11.6	0.1
		RWPB	NAB	RWPB	NAB	
Radwaste Building (RWPB) - Nuclear		51	41	7.3	10.1	2.7
Auxiliary Building (NAB)		52	40	8.7	11.4	2.6

u_v (NI) - Settlements at the end of the 8th loading step at the base of the N

u_v (Adj. Bldg)- Settlements at the end of the 8th loading step at the base of the adjacent building

Δu_v - Differential Settlements

Figure 2.5-194—{NI Tilt in Four Cross Sections Not Used}



RAI 229

Question 02.05.04-19

FSAR Section 2.5.4.10.1 states that the dynamic bearing capacity for the NI was assessed by dividing the ultimate bearing capacity obtained over a FOS of 2.0 and comparing it with the allowable capacity permitted in the U.S. EPR FSAR. Please discuss any possible deduction of bearing capacity under seismic/dynamic loadings.

Response

Earthquakes have the potential of decreasing the bearing capacity of foundations. Several studies indicate that the critical slip surface becomes shallower as the acceleration intensity increases. For this analysis, the solution proposed by Soubra (1999) is used to estimate the seismic bearing capacity of the NI common mat buildings at CCNPP Unit 3. This method is based on the solution of two failure mechanisms using the limit analysis theory. The soil is assumed as a homogeneous isotropic material and follows an associated flow rule Coulomb material obeying Hill's maximal work principle.

In the analysis, weighted average values of c' , ϕ' and γ' are used based on relative thickness of each stratum in the zone between the bottom of the footing and a depth B below this point, where B is the least lateral dimension of the building. Soil layer thickness and strength parameters are shown in Tables 17 and 18. Effective soil parameters are used (drained conditions). A horizontal acceleration coefficient of $k_h = 0.15g$ is considered in the analysis; vertical accelerations are often disregarded (Soubra, 1999) and thus they are not considered in this analysis. The weighted average strength parameters used in the analysis are $c' = 0.68$ ksf and $\phi' = 33$ degrees.

A dynamic bearing capacity analysis was performed to assess the impact of seismic forces that produce overturning moments in the foundation. During overturning, the effective supporting area is reduced, resulting in a decrease in the bearing capacity of the subsurface. To take into account this effect and simulate the potential for higher edge pressures during dynamic loading, the seismic bearing capacity is calculated for three different foundation widths: B1 = 270 ft, B2 = 203 ft, and B3 = 135 ft, which correspond to the original foundation width, and two reduced values. The reduction for B2 and B3 is 25% and 50% are considered as a sensitivity analysis. The results of the analysis are provided in Table 19.

Even if the foundation width is reduced by half (B3 = 135 ft), the allowable dynamic bearing capacity (58.5 ksf) is larger than the Areva design certification requirement of 35 ksf. For the case with average soil strength parameters and the original foundation width (B1 = 270 ft), the allowable dynamic bearing capacity is 72.9 ksf.

The dynamic bearing capacity of 72.9 ksf is lower than the allowable static bearing capacity of 87.8 ksf (Vesic method). The deduction due to seismic forces in this case is around 17%. For the same case, the deduction of ultimate static bearing capacity is approximately 45%. Lower deductions are expected for allowable bearing capacities since a smaller factor of safety is considered for the dynamic case. The factors of safety are FOS = 3 for static loading and FOS = 2 for dynamic loading.

Table 17
Stratum Thickness and Unit Weights used in the Seismic Bearing Capacity Calculation
CCNPP Unit 3 Powerblock Area

Stratum	Elevation (ft)		Thickness (ft)	Unit Weight γ (pcf)	Effective Unit Weight γ' (pcf)
	Top	Bot			
Structural fill	83.0	41.5	41.50	145	82.6
Stratum IIb-1 Chesapeake Cemented Sand	41.5	15.5	26.00	122	59.6
Stratum IIb-2 Chesapeake Cemented Sand	15.5	-7.5	23.00	123	60.6
Stratum IIb-3 Chesapeake Cemented Sand	-7.5	-23.5	16.00	123	60.6
Stratum IIc Chesapeake Clay/Silt	-23.5	-213.5	190.00	104	41.6
Stratum III Nanjemoy Sand	-213.5	-317.0	103.50	127	64.6

Table 18
Soil Strength Parameters used in the Seismic Bearing Capacity
CCNPP Unit 3 Powerblock Area

Stratum	c ' (ksf)	ϕ ' (deg)
Structural fill	0.00	40.00
Stratum IIb-1, Chesapeake Cemented Sand	0.60	34.00
Stratum IIb-2, Chesapeake Cemented Sand	0.52	32.00
Stratum IIb-3, Chesapeake Cemented Sand	0.22	32.00
Stratum IIc, Chesapeake Clay/Silt	0.80	32.00
Stratum III, Nanjemoy Sand	0.00	40.00

Table 19
Seismic Bearing Capacity Results

Dynamic Bearing Capacity	Foundation Width (ft)		
	$B_1 = 270$	$B_2 = 203$	$B_3 = 135$
Ultimate, q_{ult} (ksf)	145.8	131.9	117.0
Allowable, q_a (ksf) ⁽¹⁾	72.9	66.0	58.5

(1) Factor of safety for dynamic forces is $FOS = 2.0$. i.e., $q_a = q_{ult}/FOS$

COLA Impact

Section 2.5.4.10.1 of the CCNPP Unit 3 FSAR is revised as shown below. This revision incorporates a new table.

2.5.4.10.1 Bearing Capacity

...

A summary of the calculated allowable static and dynamic bearing capacities using both the layered and the homogeneous soil conditions are presented in Table 2.5-65. A factor of safety of 3.0 for static loads (dead plus live loads) and 2.0 for dynamic loading are typically considered to be acceptable.

Table 5.0-1 of the U.S. EPR FSAR identifies the soil bearing capacity as a required parameter to be enveloped, defined as a minimum static bearing capacity of "22,000 lb/ft² in localized areas at the bottom of the Nuclear Island basemat and 15,000 lb/ft² on average across the total area of the bottom of the Nuclear Island basemat." and a "minimum dynamic bearing capacity of 34,560 lb/ft² at the bottom of the NI basemat."

A dynamic bearing capacity analysis was performed to assess the impact of seismic forces that produce overturning moments in the foundation. During overturning, the effective supporting area is reduced, resulting in a decrease in the bearing capacity of the subsurface. To take into account this effect and simulate the potential for higher edge pressures during dynamic loading, the seismic bearing capacity is calculated for three different foundation widths: B1 = 270 ft, B2 = 203 ft, and B3 = 135 ft, which correspond to the original foundation width, and two reduced values. The reduction for B2 and B3 is 25% and 50% are considered as a sensitivity analysis of the effective bearing area. The results of the analysis are provided in Table 2.5-102.

Even if the foundation width is reduced by half (B3 = 135 ft), the allowable dynamic bearing capacity (58.5 ksf) is larger than the AREVA design certification requirement of 35 ksf. For the case with average soil strength parameters and the original foundation width (B1=270 ft), the allowable dynamic bearing capacity is 72.9 ksf.

The dynamic bearing capacity of 72.9 ksf is lower than the allowable static bearing capacity of 87.8 ksf (Vesic method). The deduction due to seismic forces in this case is around 17%. For the same case, the deduction of ultimate static bearing capacity is approximately 45%. Lower deductions are expected for allowable bearing capacities since a smaller factor of safety is considered for the dynamic case. The factors of safety are FS = 3 for static loading and FS = 2 for dynamic loading.

The static bearing capacity is above the localized 22 ksf requirement and the dynamic bearing capacity is above the 34.56 ksf requirement.

For static and dynamic loading conditions, and based on a factor of safety of 3.0 (static) and 2.0 (dynamic), the site provides adequate allowable bearing capacity.}

2.5.4.10.2 Settlement

...

Table 2.5-102 – Seismic Bearing Capacity Results

<u>Dynamic Bearing Capacity</u>	<u>Foundation Width (ft)</u>		
	<u>B₁ = 270</u>	<u>B₂ = 203</u>	<u>B₃ = 135</u>
<u>Ultimate, q_{ult} (ksf)</u>	<u>145.8</u>	<u>131.9</u>	<u>117.0</u>
<u>Allowable, q_a (ksf) ⁽¹⁾</u>	<u>72.9</u>	<u>66.0</u>	<u>58.5</u>

Notes:

(1) Factor of safety for dynamic forces is FOS = 2.0. i.e., q_a = q_{ult}/FOS